Contextual Tokenization for Graph Inverted Indices

Pritish Chakraborty IIT Bombay

Indradyumna Roy IIT Bombay

Soumen Chakrabarti IIT Bombay

Abir De IIT Bombay

Emails: {pritish, indraroy15, soumen, abir}@cse.iitb.ac.in

Abstract

Retrieving graphs from a large corpus, that contain a subgraph isomorphic to a given query graph, is a core operation in many real-world applications. While recent multi-vector graph representations and scores based on set alignment and containment can provide accurate subgraph isomorphism tests, their use in retrieval remains limited by their need to score corpus graphs exhaustively. We introduce CORGII (Contextual Representation of Graphs for Inverted Indexing), a graph indexing framework in which, starting with a contextual dense graph representation, a differentiable discretization module computes sparse binary codes over a learned latent vocabulary. This text document-like representation allows us to leverage classic, highly optimized inverted indices, while supporting soft (vector) set containment scores. Pushing this paradigm further, we replace the classical, fixed impact weight of a 'token' on a graph (such as TFIDF or BM25) with a data-driven, trainable impact weight. Finally, we explore token expansion to support multi-probing the index for smoother accuracy-efficiency tradeoffs. To our knowledge, CORGII is the first indexer of dense graph representations using discrete tokens mapping to efficient inverted lists. Extensive experiments show that CORGII provides better trade-offs between accuracy and efficiency, compared to several baselines. Code is in: `https://github.com/structlearning/corgii`.

1 Introduction

Given a query graph G_q, a common graph retrieval task is to find, from a large corpus of C graphs, graphs G_c that each contain a subgraph isomorphic to G_q [1]. The ranking relaxation is to find K graphs that 'best' contain G_q, under a suitable notion of approximate subgraph containment score. This task has several applications, *e.g.*, functional group search in molecular databases [2], control-flow pattern detection in program analysis [3], semantic search in scene graphs [4], *etc*.

Graph retrieval faces two challenges. Locally, the exact subgraph isomorphism decision problem is NP-complete [5] — but this can be circumvented via suitable score approximations, even if heuristic in nature. The more pressing global challenge is that the best approximations need early cross-interaction between G_q and G_c, leading to an impractical $\Omega(C)$ query time. Our goal is to devise a novel indexing framework to attack the global bottleneck.

Single vs. multi-vector graph representation tradeoffs Approximate scores for graph containment may be computed by two families of neural networks. Early methods [6, 7, 8] use a single vector to represent a whole graph, enabling efficient relevance computation in (hashable/indexable) Euclidean space, but miss fine-grained structural details. Later methods [9, 10, 11] represent a graph as a *set* of node embedding vectors and solve a form of optimal transport [9, 10] between them to get better score approximations. This parallels the shift in dense text retrieval from late-interaction or "dual encoder" or "bi-encoder" style that pools a passage into a single vector [12, 13, 14] to multi-vector representations [15, ColBERT].

Lessons from text retrieval Classical text retrieval used inverted indices keyed on discrete tokens or words [16, 17, 18] mapping to posting lists of document IDs, with highly optimized implementations [19, 20, 21] that are still widely used. When word embeddings and neural text encoders became popular, first-generation dense retrieval systems used single vectors to represent queries and passage,

39th Conference on Neural Information Processing Systems (NeurIPS 2025).

leading to rapid adoption of approximate nearest neighbor (ANN) indexing methods [22, 23, 24, 25, 26, 27, 28, 29, 30, 31, 32, 33, 34].

Mirroring the situation with graphs, late interaction between query and passage embeddings via cosine, L2 or dot product scores leads to efficient indices, but these scores are not as accurate as those obtained by early cross-interaction, which are not directly indexable. A notable and effective compromise was separate contextualization of query and passage words, followed by a novel *Chamfer score* [35] as an indexable surrogate of cross-interaction, as in ColBERT [15] and PLAID [36]. These methods probe the ANN index once per query word, and perform extra decompression and bookkeeping steps for scoring passages. Thus, even the partial contextualization and limited cross-interaction come at a performance premium. SPLADE [37] further improves efficiency by pre-expanding documents to include extra related words, and then use a standard inverted index on these expanded documents. In case of text, contextual similarity between words provides the signals needed for expansion.

1.1 Our Contributions

In proposing our system, CORGII (Contextual Representation of Graphs for Inverted Indexing), our goal is to apply the wisdom acquired from the recent history of dense text retrieval to devise a scalable index for graphs to support subgraph containment queries. In doing so, we want to use a contextual graph representation that gives accurate containment scores, but also takes advantage of decades of performance engineering invested in classic inverted indices.

Differentiable graph tokenization We introduce a graph tokenizer network (GTNet) which uses a graph neural network (GNN) to map each node to a structure-aware token over a latent vocabulary. At the outset, GTNet computes binary node representations, which serve as discrete tokens, thereby forming multi-vector discrete graph representations. Our approach is significantly different from existing continuous graph embedding methods [6, 7, 9, 10, 8, 11], most of which employ Siamese networks with hinge distance to learn order embeddings. In contrast, inverted indices basically implement fast sparse dot-product computation. To reconcile this gap, we use separate tokenizer networks for query and corpus graphs, but allow a symmetric distance between the matched nodes.

Prior works [9, 10] also use injective alignment. However, we find it suboptimal, due to the subtle inconsistencies introduced by its continuous relaxation. Instead, we compute the Chamfer distance [35] over discrete node representations, which supports accurate token matching, even without injective alignment. We use these tokens to build an inverted index, where each token is mapped to the posting lists of corpus graphs containing it.

Query-aware trainable impact score Text queries and documents represented as pure word sets (ignoring word counts or rarity) are not as effective for retrieval as *vector space models*, where each word has a certain *impact* on the document, based on raw word frequency, rarity of the word in the corpus (inverse document frequency or IDF), etc. Thus the query and each document are turned into sparse, non-negative, real-valued vectors.

We introduce a trainable token impact score that acts as a learned analog of classical term weights like TFIDF and BM25, but for tokenized graphs instead of text. Given a query node, this score function takes as input both its continuous and discrete representation and assigns different importance weights to the same words based on the structural information, captured through the continuous representation. This enables fine-grained, query-aware scoring while maintaining compatibility with inverted indexing.

Recall-enhancing candidate generation prior to reranking Identifying the best match for a query node in a corpus graph typically requires global optimization over all nodes. In contrast, inverted indexing performs independent per-node matching, often leading to false positives. To tackle this problem, we introduce a novel co-occurrence based multiprobing strategy, where, given a token, we probe other tokens with large overlap between their posting lists. Finally, we perform a thresholded aggregation, which facilitates smooth, tunable control over the trade-off curve between accuracy and efficiency.

Experiments on several datasets show that CORGII is superior to several baselines. Moreover, the design of CORGII naturally enables a smooth trade-off between query latency and ranking quality, which is critical in many applications.

2 Preliminaries

Notation. We denote $G_q = (V_q, E_q)$ as a query graph and $G_c = (V_c, E_c)$ as a corpus graph. Let $\{G_1, G_2, ..., G_C\}$ be the set C corpus graphs. Each query-corpus pair (G_q, G_c) is annotated with a binary label $y_{qc} \in \{0, 1\}$, where $y_{qc} = 1$ iff $G_q \subseteq G_c$. Given corpus item indices $\mathcal{C} = [C] = \{1, .., C\}$, we define the set of relevant graphs as $\mathcal{C}_{q\oplus} = \{c : \mid y_{qc} = 1\}$ and the set of non-relevant graphs as $\mathcal{C}_{q\ominus} = \mathcal{C} \backslash \mathcal{C}_{q\oplus}$. Assuming $|V_q| = |V_c| = m$ obtained after suitable padding, we write $\boldsymbol{A}_q, \boldsymbol{A}_c \in \{0, 1\}^{m\times m}$ as the adjacency matrices for G_q and G_c respectively. $[\bullet]_+ = \max\{0, \bullet\}$ is the ReLU or hinge function. $[\![\bullet]\!]$ denotes the indicator function which is 1 if predicate $\bullet$ holds and 0 if it does not.

Subgraph isomorphism Given G_q and G_c, the subgraph isomorphism problem seeks to determine iff $G_q \subseteq G_c$. This is equivalent to checking whether there exists a permutation matrix $\boldsymbol{P}$ such that $\boldsymbol{A}_q \le \boldsymbol{P}\boldsymbol{A}_c\boldsymbol{P}^\top$, which results in a coverage loss based relevance distance, defined as: $\min_{\boldsymbol{P}\in\mathcal{P}_m}[\boldsymbol{A}_q - \boldsymbol{P}\boldsymbol{A}_c\boldsymbol{P}^\top]_+$.

Computation of $\Delta(G_q, G_c)$ defined above requires solving a quadratic assignment problem (QAP), which is NP-hard. Therefore, existing works [9, 10] propose a differentiable surrogate of this QAP using an asymmetric set distance. Given G_q and G_c, they employ a graph neural network (GNN) to compute the node embeddings $\boldsymbol{h}_q(u), \boldsymbol{h}_c(v) \in \mathbb{R}^{\text{dim}_h}$ for $u \in V_q$ and $v \in V_c$ respectively, then collect them in $\boldsymbol{H}_q \in \mathbb{R}^{m\times\text{dim}_h}$ and $\boldsymbol{H}_c \in \mathbb{R}^{m\times\text{dim}_h}$, where m is the number of nodes (after padding). These embeddings are fed into a Gumbel-Sinkhorn network [38, 39], which produces a doubly stochastic matrix $\boldsymbol{P}$ — a relaxed surrogate of the binary permutation matrix — thus providing an approximate, injective node alignment map. This enables an approximation of $\min_{\boldsymbol{P}\in\mathcal{P}_N}[\boldsymbol{A}_q - \boldsymbol{P}\boldsymbol{A}_c\boldsymbol{P}^\top]_+$ as the following surrogate relevance distance:

$$\Delta(G_q, G_c) = \textstyle\sum_{i\in[\text{dim}_h], u\in[m]}[\boldsymbol{H}_q - \boldsymbol{P}\boldsymbol{H}_c]_+[u, i], \quad \boldsymbol{P} \in [0, 1]^{m\times m} \text{ is doubly stochastic.} \tag{1}$$

The underlying GNN and Gumbel-Sinkhorn network is trained under the distant supervision of binary relevance labels, without any demonstration of ground truth permutation matrix $\boldsymbol{P}$. We shall regard $\boldsymbol{H}_q, \boldsymbol{H}_c$ and Eqn. (1) as references to compute final scores of qualifying candidates that survive our index probes.

Pretrained backbone We use an existing subgraph matching model, namely IsoNet [9], which provides a relevance distance $\Delta(G_q, G_c)$ of the form given in Eq. (1) for any query-corpus graph pair (G_q, G_c). This pre-trained backbone is employed solely at the final stage to compute $\Delta(G_q, G_c)$ for ranking the retrieved candidates. Therefore, we can access $\boldsymbol{H}_q, \boldsymbol{H}_c$ and the corresponding node alignment map $\boldsymbol{P}$.

Inverted Index Here, we describe inverted index based retrieval in a general information retrieval setting with query q and corpus objects wih IDs $\mathcal{C} = \{1, ..., C\}$. Given a vocabulary ω, we represent each instance c by a set of discrete tokens $\omega(c) = \left\{\tau^{(1)}, \tau^{(2)}, \ldots\right\}$, where each $\tau^{(\bullet)} \in \omega$. For a collection of corpus items $\mathcal{C}$, the inverted index maps each token in ω to the set of corpus items containing it. Specifically, each token τ is associated with a posting list $\text{PostingList}(\tau)$, which consists of all $c \in \mathcal{C}$ containing τ, *i.e.*, $\omega(c) \ni \tau$. Formally, we write $\text{PostingList}(\tau) = \text{List}(\{\tau \mid \tau \in \omega(c)\})$. In "impact-ordered" posting lists, corpus items are sorted in decreasing order of "impact scores" that capture the importance of a word in a document. Typically, in text retrieval, impact scores are modeled using term frequency (TF) and inverted document frequency (IDF) [17]. Given a query x_q, we obtain the token set $\omega(q)$ and then probe the inverted index to traverse across the posting list of each token $\tau \in \omega(q)$. Finally, we retrieve candidates from all such posting lists and return a subset from them as top-k candidates.

3 Proposed approach

We now present CoRGII: a scalable retrieval system for graph retrieval that takes advantage of decades of optimization of inverted indices on discrete tokens, and yet supports scoring and ranking using continuous node embeddings. Starting with the hinge distance (1), we propose a series of steps that adapt GNN-based contextual node embeddings toward a discrete token space, enabling us to use inverted indices. Before describing the modules of CoRGII, we outline these adaptation steps.

GNN-based node embeddings As described in Section 2, a (differentiable) GNN contextualizes nodes in their graph neighborhood to output $\{\boldsymbol{x}_q(u)\}$ and $\{\boldsymbol{x}_c(v)\}$. The (transportation-inspired) hinge distance between them, found effective for ranking in earlier work, is asymmetric and based

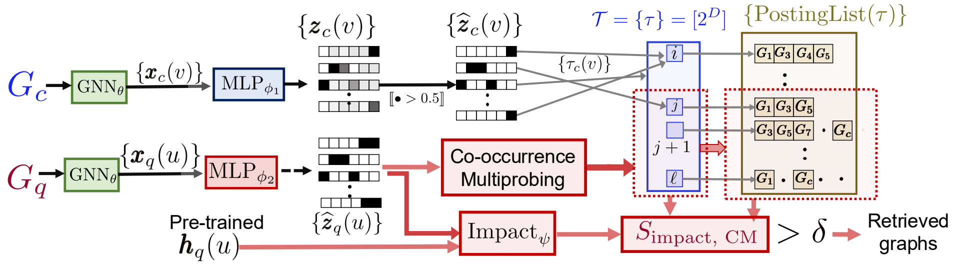

Figure 1: CoRGII block diagram. Each (query, corpus) graph pair (G_q, G_c) is encoded using a shared GNN$_\theta$, followed by separate MLPs (MLP$_{\phi_1}$ and MLP$_{\phi_2}$) to compute soft binary node embeddings $\boldsymbol{z}_c(v), \boldsymbol{z}_q(u) \in (0,1)^D$. These are thresholded to obtain discrete binary codes $\widehat{\boldsymbol{z}}_c(v), \widehat{\boldsymbol{z}}_q(u) \in \{0,1\}^D$, mapped to integer-valued latent tokens $\tau \in \mathcal{T} = [2^D]$. Corpus tokens are indexed into posting lists $\text{PostingList}(\tau)$, enabling sparse inverted indexing. During retrieval, query tokens $\tau_q(u)$ are expanded via co-occurrence–based multi-probing (CM) to select similar tokens $\mathcal{N}_b(\tau_q(u))$. Each expanded token τ contributes to the corpus score through an impact score $\text{Impact}_\psi(\tau, \boldsymbol{h}_q(u))$, producing the overall retrieval score $S_{\text{impact,CM}}(G_q, G_c)$. Graphs with score exceeding a threshold δ are shortlisted and reranked using the alignment distance $\Delta(G_q, G_c)$ (Eq. (1)).

on a (soft) permutation $\boldsymbol{P}$. These introduce two major hurdles in the way of deploying inverted indices. CoRGII approximates the asymmetric, early-interaction distance (1) with an asymmetric dual encoder (late interaction) network, but based on a non-injective granular scoring function.

Efficient differentiable (near-)tokenization As a first step toward tokenization, we apply two (still differentiable, but distinct) networks to $\boldsymbol{x}_q(u), \boldsymbol{x}_c(v)$, ending with sigmoid activations, which take the outputs $\boldsymbol{z}_q(u), \boldsymbol{z}_c(v)$ closer to bit-vector representation of tokens. The GNN, together with these networks, are trained for *retrieval accuracy* (and not, *e.g.*, any kind of reconstruction). We also replace the permutation with a Chamfer distance [35] which brings us closer to inverted indices.

Token discretization and indexing Finally, we round $\boldsymbol{z}_q(u), \boldsymbol{z}_c(v)$ to 0/1 bit vectors $\widehat{\boldsymbol{z}}_q(u), \widehat{\boldsymbol{z}}_c(v)$, assigning a bit-vector token to each node. Much like text documents, a graph is now represented as a multiset of discrete tokens. With this step, we lose differentiability, but directly use an inverted index.

Impact weights and multi-probing All tokens should not contribute equally to match scores. Based on corpus and query workloads, we learn suitable impact weights of these (manufactured) tokens. We further optimize the performance of CoRGII by designing a suitable aggregation mechanism to prune the posting lists obtained from all the query tokens. Finally, we consider one folklore and one novel means to explore the 'vicinity' of a query token, to provide a smooth trade-off between query latency and ranking accuracy.

3.1 Graph tokenizer network GTNet

We now proceed to describe the major components of CoRGII.

The first stage of GTNet is a standard GNN similar to that described in Section 2, but here we will train it exclusively for indexing and retrieval. The GNN will share the same parameters θ across query and corpus graphs. After the GNN, we will append a multi-layer perceptron (MLP) layer with different parameters ϕ_1 and ϕ_2 for the query and corpus graphs.

$$\boldsymbol{z}_q(u) = \sigma(\text{MLP}_{\phi_1}(\boldsymbol{x}_q(u))) \;\text{ for } u \in V_q \quad \text{where, } \{\boldsymbol{x}_q(u)\} = \text{GNN}_\theta(G_q); \tag{2}$$

$$\boldsymbol{z}_c(v) = \sigma(\text{MLP}_{\phi_2}(\boldsymbol{x}_c(v))) \;\text{ for } v \in V_c \quad \text{where, } \{\boldsymbol{x}_c(v)\} = \text{GNN}_\theta(G_c). \tag{3}$$

Rationale behind different MLP networks Unlike exact graph matching, the subgraph matching task is inherently asymmetric, where $G_q \subset G_c$ does not mean $G_c \subset G_q$. To model this asymmetry, existing works [7, 9, 10] employs hinge distance $\Delta(G_q, G_c)$ (1), while sharing a a Siamese network with the same parameters for query and corpus pairs. However, such approach will preserve subgraph matching through order embeddings: $\boldsymbol{Z}_q \leq \boldsymbol{S}\boldsymbol{Z}_c$. But inverted indexing requires exact token matching, making order embeddings incompatible with token-based indexing. Therefore, we retain asymmetry through separate MLPs for queries and corpus.

Introducing Chamfer Distance between graphs An asymmetric Siamese network lets us replace hinge distance $[\boldsymbol{H}_q - \boldsymbol{P}\boldsymbol{H}_c]_+$ with the normed distance $\|\boldsymbol{Z}_q - \boldsymbol{P}\boldsymbol{Z}_c\|_1$, but, for the sake of indexing, we need to avoid the permutation $\boldsymbol{P}$ (whose best choice depends on both $\boldsymbol{H}_q$ and $\boldsymbol{H}_c$), so that 'document' graphs can be indexed independent of queries. Moreover, training from relevance labels require $\boldsymbol{P}$ to be modeled as a doubly stochastic soft permutation matrix (see Eq. (1)). However, its continuous nature of $\boldsymbol{P}$ smears the values in $\boldsymbol{Z}_q$ and $\boldsymbol{Z}_c$, leading to poor discretization. Due to these reasons, we avoid the permutation, and for each query node u, match $\boldsymbol{z}_q(u)$ to $\boldsymbol{z}_c(v)$ for some corpus node v, *independently of other query nodes*, as opposed to the joint matching of all nodes in query corpus pairs, thus permitting non-injective mappings via the *Chamfer distance* [35]:

$$\text{Chamfer}(G_q, G_c) = \textstyle\sum_{u \in V_q} \min_{v \in V_c} \|\boldsymbol{z}_q(u) - \boldsymbol{z}_c(v)\|_1, \tag{4}$$

Ideally, relevant graphs yield $\text{Chamfer}(G_q, G_c) = 0$, but GTNet produces approximate binary representations, making exact matches unlikely. To ensure a robust separation between the relevant and non-relevant query-corpus pairs, we seek to impose a margin of separation m: non-relevant graphs should differ by at least one additional bit per node compared to the relevant graphs, corresponding to a total Chamfer distance separation of m.

Formally, for a query graph G_q, and the set of relevant and irrelevant (or less relevant) corpus graphs $c_\oplus \in \mathcal{C}_{q\oplus}$ and $c_\ominus \in \mathcal{C}_{q\ominus}$, we require $\text{Chamfer}(G_q, G_{c_\oplus}) + m < \text{Chamfer}(G_q, G_{c_\ominus})$. This yields the following ranking loss optimized over parameters of GTNet, *i.e.*, θ, ϕ_1, ϕ_2:

$$\min_{\theta,\phi_1,\phi_2} \sum_q \sum_{c_\ominus \in \mathcal{C}_{q\ominus}, c_\oplus \in \mathcal{C}_{q\oplus}} [\text{Chamfer}(G_q, G_{c_\oplus}) - \text{Chamfer}(G_q, G_{c_\ominus}) + m]_+ \tag{5}$$

Note that node embeddings $\boldsymbol{Z}_q, \boldsymbol{Z}_c$ still allow backprop, but are closer to "bit vectors". Moreover, the training of θ, ϕ_1, ϕ_2 is guided not by reconstruction considerations, but purely by retrieval efficacy.

3.2 Discretization and inverted index

Once GTNet is trained, we compute, for each corpus graph and node therein, $\boldsymbol{z}_c(v)$, and, from there, a bit vector $\widehat{\boldsymbol{z}}_c(v) = [\![\boldsymbol{z}_c(v) > 0.5]\!]$ as a 'hard' representation of each corpus node (and similarly from $\boldsymbol{z}_q(u)$ to $\widehat{\boldsymbol{z}}_q(u)$ for query nodes u). Given $\boldsymbol{z}_c(v) \in (0,1)^D$, this means $\widehat{\boldsymbol{z}}_c(v) \in \{0,1\}^D$, *i.e.*, each node gets associated with a D-bit integer. Let us call this the *token space* $\mathcal{T} = [2^D]$. Note that multiple nodes in a graph may get assigned the same token. Thus, each query graph G_q and corpus graph G_c are associated with *multisets* of tokens, denoted

$$\omega(G_q) = \{\!\{\widehat{\boldsymbol{z}}_q(u) : u \in V_q\}\!\} \quad \text{and} \quad \omega(G_c) = \{\!\{\widehat{\boldsymbol{z}}_c(v) : v \in V_c\}\!\}. \tag{6}$$

(If a graph is padded for efficient tensor operations, the tokens corresponding to padded nodes are logically excluded from the multisets. We elide this code detail for clarity.)

Conceptually, a basic inverted index is a map where the keys are tokens. Each token $\tau \in \mathcal{T}$ is mapped to the set (without multiplicity) of corpus graphs (analog of 'documents') in which it appears: $\text{PostingList}(\tau) = \{c \in \mathcal{C} : \tau \in \omega(G_c)\}$. Intuitively, the goal of minimizing the Chamfer distance (4) in the pre-discretized space corresponds, in the post-discretized space, to locating documents that have large token overlap with the query, which finally enables us to plug in an inverted index.

Candidate generation using uniform impact At query time, the query graph G_q is processed as in (6), to obtain $\omega(G_q)$. Given the inverted index, each token $\tau \in \omega(G_q)$ is used to retrieve $\text{PostingList}(\tau)$. As a simple starting point (that we soon improve), a corpus graph can be scored as

$$S_{\text{unif}}(G_q, G_c) = \textstyle\sum_{u \in V_q} [\![\widehat{\boldsymbol{z}}_q(u) \in \omega(G_c)]\!]. \tag{7}$$

(If multiple nodes u have the same token $\widehat{\boldsymbol{z}}_q(u)$, they are counted multiple times. Belongingness in $\omega(G_c)$ is Boolean, without considering multiplicities.) These scores are used to select a subset of candidates from the whole corpus. These qualifying candidates are reranked using the (computationally more expensive) alignment-based distance $\Delta(G_q, G_c)$ (1).

3.3 Impact weight network

The crude unweighted score (7) has some limitations: (1) Information is lost from $\boldsymbol{H}$ to $\boldsymbol{Z}$ to $\hat{\boldsymbol{Z}}$. Nodes with minor differences in neighborhood structure may be mapped to overlapping tokens, resulting in large candidate pools. (2) Similar to IDF, we need to discriminate against common graph motifs with poor selectivity. In our setting, the combinatorial explosion of motifs makes the estimation of motif frequencies intractable [40]. Moreover, unlike IDF in text retrieval [17], frequent structures cannot be down-weighted, as subgraph retrieval requires matching all query components, regardless of the frequency of the subgraphs.

To mitigate the above difficulties, we use a notion of token impact weight in the same spirit as in traditional text retrieval, although there are some crucial differences. We introduce an *impact weight network* $\text{Impact}_\psi : \mathcal{T} \times \mathbb{R}^{\dim_h} \to \mathbb{R}$, parameterized with ψ, where $\dim_h$ is the dimension of the

(a) 2-stage training of CoRGII

```
input: graph corpus $\mathcal{C}$, training queries $\{G_q\}$ with relevance labels $\{y_{qc}\}$
▷ Train GTNet ◁
for each query-corpus pair $(G_q, G_c)$ do
    Compute $\boldsymbol{Z}_q = \text{GTNet}(G_q)$ (Eq. (2))
    Compute $\boldsymbol{Z}_c = \text{GTNet}(G_c)$ (Eq. (3))
    Compute $\text{Chamfer}(G_q, G_c)$ (Eq. (4))
Train GTNet by minimizing margin-based ranking loss on $\text{Chamfer}(G_q, G_c)$ (Eq. (5))
▷ Train impact network ◁
for each query-corpus pair $(G_q, G_c)$ do
    Compute $\boldsymbol{Z}_q = \text{GTNet}(G_q)$
    ▷ Compute binary embeddings ◁
    $\{\widehat{\boldsymbol{z}}_q(u)\} = [\![\boldsymbol{Z}_q > 0.5]\!]$
    ▷ compute impact scores of all query graphs ◁
    compute $S_{\text{impact}}(G_q, G_c)$ (Eq. (9))
Train $\text{Impact}_\psi$ network by minimizing margin-based ranking loss on $S_{\text{impact}}(G_q, G_c)$ (Eq. (10))
```

(b) Retrieval and reranking

```
inputs: query $G_q$, threshold $t$, pre-trained embeddings $\{\boldsymbol{h}_q(u)\}$ for $G_q$.
▷ Obtain approximate binary representation ◁
Compute $\boldsymbol{Z}_q = \text{GTNet}(G_q)$ (Eq. (2))
▷ Compute binary embeddings and tokens ◁
$\{\widehat{\boldsymbol{z}}_q(u)\} = [\![\boldsymbol{Z}_q > 0.5]\!]$
$\omega(G_q) = \text{ObtainTokenSet}(\{\widehat{\boldsymbol{z}}_q(u)\})$
▷ Compute impact weights ◁
for each node $u \in V_q$ do
    Compute $\text{Impact}_\psi(\widehat{\boldsymbol{z}}_q(u), \boldsymbol{h}_q(u))$ (Eq. (8))
▷ Probe index using query node tokens and their impacts (with optional token expansion) and aggregate preliminary relevance scores ◁
$S_{\text{impact},CM}(G_q, G_c)$ (Eq. (9))
▷ Shortlist candidates ◁
$\mathcal{R}_q(\delta) = \{G_c : S_{\text{impact},CM}(G_q, G_c) \geq \delta\}$ (11)
rerank surviving candidates using $\Delta(G_q, G_c)$ (1)
return top-$k$ corpus graphs
```

Figure 2: (a) preprocessing and (b) query-time components of CoRGII.

pre-trained continuous node embedding $\boldsymbol{h}_q(\bullet)$ or $\boldsymbol{h}_c(\bullet)$. We often substitute τ with $\widehat{\boldsymbol{z}}_q(u)$ in the input to Impact_ψ depending on context.

Neural architecture of Impact_ψ Network Impact_ψ is implemented as a lightweight multi layer perceptron (MLP). Given input token τ, presented as a binary code from $\{0,1\}^D$, and input node embedding $\boldsymbol{h}$, we concatenate them and pass the result through a multi-layer perceptron, *i.e.*,

$$\text{Impact}_\psi(\tau, \boldsymbol{h}) = \text{MLP}_\psi\left(\text{concat}\left(\tau, \boldsymbol{h}\right)\right). \tag{8}$$

Rather than count all matched tokens uniformly (7), we compute an impact-weighted aggregate:

$$S_{\text{impact}}(G_q, G_c) = \sum_{u \in V_q} \text{Impact}_\psi(\widehat{\boldsymbol{z}}_q(u), \boldsymbol{h}_q(u)) \, [\![\widehat{\boldsymbol{z}}_q(u) \in \omega(G_c)]\!] \tag{9}$$

Thus, token matches are weighted according to their learned structural importance rather than treated uniformly, enabling fine-grained, query-sensitive retrieval over the inverted index.

Training Impact_ψ Let $\mathcal{C}_{q\oplus}$ and $\mathcal{C}_{q\ominus}$ be the relevant and non-relevant graphs for query G_q. Similar to Eq. (5), we encourage that $S_{\text{Impact}}(G_q, G_{c_\oplus}) > S(G_q, G_{c_\ominus}) + \gamma$ for $c_\oplus \in \mathcal{C}_{q\oplus}$ and $c_\ominus \in \mathcal{C}_{q\ominus}$, where $\gamma > 0$ is a margin hyperparameter. As before, this leads to a pairwise hinge loss to train ψ:

$$\underset{\psi}{\text{argmin}} \sum_q \sum_{c_\oplus \in \mathcal{C}_{q\oplus}} \sum_{c_\ominus \in \mathcal{C}_{q\ominus}} \left[S_{\text{impact}}(G_q, G_{c_\ominus}) - S_{\text{impact}}(G_q, G_{c_\oplus}) + \gamma\right]_+. \tag{10}$$

Note that the networks described earlier, with parameters θ, ϕ_1, ϕ_2 are frozen before training the impact parameters ψ. Unlike in classical inverted indices, impact weights are not associated with documents, or stored in the index. Figure 2(a) shows all the training steps of CoRGII.

3.4 Query processing steps and multi-probing

At retrieval time, the query graph G_q is first embedded using the pretrained encoder $\mathcal{E}$ to obtain node embeddings $\boldsymbol{H}_q$. The graph tokenizer GTNet then discretizes $\boldsymbol{H}_q$ into soft binary codes $\boldsymbol{Z}_q$ and later hard binary codes $\hat{\boldsymbol{Z}}$, and Impact_ψ computes impact weights (if used).

Each query graph token is used to probe the inverted index. Candidate corpus graphs are retrieved by aggregating impact scores across matching tokens. Graphs with cumulative relevance scores above a tunable threshold δ form the shortlist:

$$\mathcal{R}_q(\delta) = \{c \in \mathcal{C} : S_{\spadesuit}(G_q, G_c) \geq \delta\}, \tag{11}$$

where $\spadesuit \in \{\text{unif}, \text{impact}\}$. Here, δ controls the trade-off between the query time and retrieval accuracy. High δ results in smaller size of $\mathcal{R}_q(\delta)$, yielding low query time, whereas a low δ gives high query time. Note that, $S_{\spadesuit}(G_q, G_c)$ is used only to obtain $\mathcal{R}_q$. Candidates in $\mathcal{R}_q$ are further reranked using the pretrained alignment-based 'true' distance $\Delta(G_q, G_c)$ (1). Details are in Figure 2(b).

Limitation of single probe per query node We have described how candidate corpus graphs are scored using uniform and impact-weighted aggregates. In both methods, each token $\widehat{\boldsymbol{z}}_q(u)$ from the query resulted in exactly one probe into the index. Preliminary experiments suggested that a single probe using each query token leads to lost recall, brought on partly by losing signal from continuous to bit-like node representations, and by replacing permutation-based node alignment with Chamfer score. We must discover and exploit affinities between tokens while accessing posting lists.

In the rest of this section, we explore two means to this end. The first, Hamming expansion, has already been used in the literature on locality-sensitive hashing. The second, co-occurrence expansion, is a proposal novel to CoRGII.

Term weighting	Single Probe	Hamming multiprobe (HM)	Co-occurrence multiprobe (CM)
Uniform	S_{unif}	$S_{\text{unif,HM}}\ (r = \ldots)$	$S_{\text{unif,CM}}\ (b = \ldots)$
Impact	S_{impact}	$S_{\text{impact,HM}}\ (r = \ldots)$	$S_{\text{impact,CM}}\ (b = \ldots)$ (CoRGII)

Table 3: Possible combinations of term weighting and probing strategies. Default CoRGII corresponds to $S_{\text{impact,CM}}$. r and b indicate Hamming radius for HM and number of tokens chosen for CM.

Hamming expansion multiprobe (HM) While exact token matches may be adequate when query and corpus graphs are locally near-isomorphic, discretization errors and structural noise can cause relevant corpus graphs to be missed if no exact token match is found. To improve recall, we "smooth the boundaries of token bit encodings" by introducing a lightweight *token expansion* mechanism: given a query token $\tau \in \mathcal{T}$, we probe the inverted index using not only τ, but also nearby tokens within a Hamming ball of radius r in the binary space $\{0,1\}^D$. Given $\widehat{\boldsymbol{z}}$ and $\widehat{\boldsymbol{z}}$ are the corresponding binary vectors of τ, τ' respectively, we write $B_r(\tau) = \{\tau' : \|\boldsymbol{z} - \boldsymbol{z}'\|_1 \le r\}$. S_{impact} from (9) is extended, by summing over the ball, to

$$S_{\text{impact,HM}}(G_q, G_c) = \sum_{u \in V_q} \sum_{\tau \in B_r(\widehat{\boldsymbol{z}}_q(u))} \text{Impact}_\psi(\tau, \boldsymbol{h}_q(u)) \, [\![\tau \in \omega(G_c)]\!]. \tag{12}$$

This expansion allows retrieval of corpus graphs containing *approximate matches*, mitigating the brittleness of hard discretization without requiring dense alignment. Hamming expansion has the potential to improve recall, but there is a risk of too many false positive candidates to eliminate through expensive scoring later.

Co-occurrence expansion multiprobe (CM) In classical text indexing, a token is sometimes characterized by the set of documents that mention it. Two tokens can then be compared by comparing their respective posting lists. A large overlap in these posting lists hints that the tokens have high affinity to each other. Adapting this idea to graph indexing can provide an alternative to Hamming-based affinity, which can be used either by itself, or in conjunction with Hamming-based token expansion.

For each query token $\tau \in \mathcal{T}$, we identify additional tokens τ' whose posting lists overlap significantly with the posting list of τ, *i.e.*, $\text{PostingList}(\tau)$. Specifically, we define a similarity score between tokens τ and τ' as

$$\text{sim}(\tau, \tau') = \frac{|\text{PostingList}(\tau) \cap \text{PostingList}(\tau')|}{\sum_{\tau_\star \in \mathcal{T}} |\text{PostingList}(\tau) \cap \text{PostingList}(\tau_\star)|} \tag{13}$$

and expanded token set $\mathcal{N}_b(\tau) = \text{argmax}^{(b)}_{\tau' \in \mathcal{T}} \text{sim}(\tau, \tau')$, where b is the number of similar tokens. Similar to Impact_ψ, we overload the input notation for sim where necessary. S_{impact} from (9) is then updated to aggregate over this expanded neighborhood, weighted by similarity:

$$S_{\text{impact,CM}}(G_c, G_q) = \sum_{u \in V_q} \sum_{\tau \in \mathcal{N}_b(\widehat{\boldsymbol{z}}_q(u))} \text{sim}(\tau, \widehat{\boldsymbol{z}}_q(u)) \, \text{Impact}_\psi(\tau, \boldsymbol{h}_q(u)) \, [\![\tau \in \omega(G_c)]\!]. \tag{14}$$

This way, a corpus graph G_c can receive a non-zero score for a query node u, if any token τ in the expanded set $\mathcal{N}_b(\boldsymbol{z}_q(u))$ appears in $\omega(G_c)$ — not just $\boldsymbol{z}_q(u)$ itself. Table 3 lists different variants including CoRGII.

4 Experiments

We assess the effectiveness of CoRGII against several baselines on real-world graph datasets and analyze the effect of different components of CoRGII. Appendix G contains additional experiments.

Dataset We evaluate CoRGII on four datasets from the TU benchmark suite [41]: PTC-FR, PTC-FM, COX2, and PTC-MR, which are also used existing works on graph matching [9, 10].

Baselines We compare CoRGII against six baselines as follows: **(1) FourierHashNet (FHN)** [42]: It is an LSH for shift-invariant asymmetric distance, computed using distance spe-

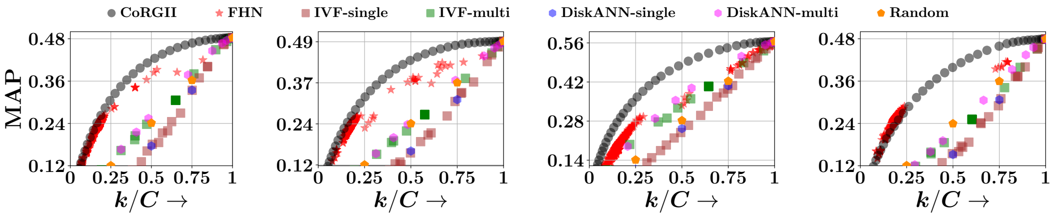

(a) PTC-FR (b) PTC-FM (c) COX2 (d) PTC-MR

Figure 4: Tradeoff between retrieval accuracy and efficiency for CoRGII, FHN [42], IVF-single [25], IVF-multi [25], DiskANN-single [29], DiskANN [29] and Random, on 20% test queries on all four datasets. Here, retrieval accuracy is measured in terms of mean average precision (MAP) and efficiency is measured as fraction of corpus graphs retrieved (k/C).

cific Fourier transform. It takes single vector graph embeddings as $\boldsymbol{a}_q = \sum_{u \in V_q} \boldsymbol{h}_q(u)/|V_q|$ and $\boldsymbol{a}_c = \sum_{v \in V_c} \boldsymbol{h}_c(v)/|V_c|$ as input and builds LSH buckets for the corpus graphs $\mathcal{C}$. **(2) IVF-single**: It is a variant of IVF [25], used for single vector retrieval. Here, we build the inverted index using single vector dense corpus representations $\{\boldsymbol{a}_c\}$ and perform retrieval by probing once with $\boldsymbol{a}_q$. **(3) IVF-multi**: It is a *multi-vector* variant of IVF [25], similar to [15, ColBert]. Here, we build the index over individual node embeddings from all corpus graphs, each tagged with its parent graph ID. During retrieval, we probe the inverted index with each query node embedding and aggregating the hits by the corresponding graph IDs. **(4) DiskANN-single** [29]: It is graph-based ANN that uses HNSW index, over single vector representations. **(5) DiskANN-multi** [29]: It is a multi-vector variant of DiskANN analogous to IVF-multi. Note that IVF and DiskANN typically support L_2 or cosine distance. We report the results for the best performing metric. **(6) Random**: Here, we select top-k items from $\mathcal{C}$ uniformly at random without replacement.

Evaluation Given the set of queries $\mathcal{Q}$ and the set of corpus graphs $\mathcal{C}$, we split $\mathcal{Q}$ in 60:20:20 train ($\mathcal{Q}_{\text{train}}$), dev ($\mathcal{Q}_{\text{dev}}$) and test ($\mathcal{Q}_{\text{test}}$) folds. For each query in $\mathcal{Q}_{\text{test}}$, we retrieve the corpus graphs $\mathcal{R}_q$ that are marked relevant by the corresponding model. We rerank the retrieved candidates using the pretrained ranking model (1). For each ranked list, we compute average precision (AP) and average the AP values across test queries $\mathcal{Q}_{\text{test}}$ to report on mean average precision (MAP). Given an accurate ranking model, MAP typically improves as the size of the candidate set $\mathcal{R}_q$ increases— larger sets are more likely to hit most of the relevant items, whereas smaller sets may miss many of them. To evaluate this trade-off between retrieval quality and efficiency, we measure MAP vs. the average size of the retrieved set, computed as $k = \frac{1}{|\mathcal{Q}_{\text{test}}|} \sum_{q \in \mathcal{Q}_{\text{test}}} |\mathcal{R}_q|$. To generate this trade-off curve, for FHN, we sweep over its training hyperparameters to learn multiple hashcode variants, and vary the number of hash table buckets during lookup. The implementations of IVF and DiskANN accept k as input. For these baselines, we directly vary k to obtain the trade-off. Appendix F report the details datasets, baselines and evaluations.

Hyperparameters We set $D = 10$, yielding the size of the vocabulary $|\mathcal{T}| = 2^{10}$, $b = 32$ in the expanded token set $\mathcal{N}_b(\widehat{\boldsymbol{z}}_q(u))$ used in co-occurrence based multi-probing (CM) in Eq. (14).

4.1 Results

CoRGII vs. baselines We first measure retrieval accuracy (MAP) and efficiency (inversely related to the fraction of corpus retrieved, k/C) across four datasets. Each curve shows how performance scales as the top-k retrieved candidates vary. Figure 4 summarizes the results. We make the following observations.

(1) CoRGII achieves the best accuracy-efficiency trade-offs among all methods. While FHN is the strongest among the baselines, CoRGII shows particularly large gains in the high-MAP regime. For example, on the COX2 dataset, CoRGII achieves a MAP of ∼0.50 at $k/C = 0.5$, whereas FHN saturates around 0.35. **(2)** Across all datasets, CoRGII achieves high MAP, very quickly at significantly lower retrieval budgets. For example, on PTC-FR, CoRGII attains a MAP of ~ 0.36 by retrieving less than $k = 33\%$ corpus graphs, while most baselines require more than 75% of the corpus to match that level.

(3) Multivector variants of IVF and DiskANN outperform their single-vector counterparts, highlighting the benefit of retaining node-level granularity. However, they still perform poorly compared to

CoRGII, largely due to their reliance on symmetric distance functions, which are unsuitable for subgraph matching — a task inherently asymmetric in nature. Single-vector variants perform the worst, sometimes even below the Random baseline, due to both the coarse nature of single-vector representations and use of symmetric distance.

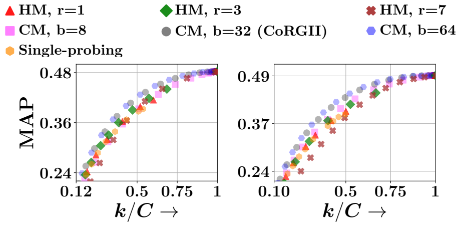

(a) PTC-FR (b) PTC-FM

Figure 5: Multiprobing: CM vs. HM

Benefits of co-occurrence based multi-probing Here, we analyze the effect of co-occurence based multiprobing (CM) strategy (14), by comparing it with a traditional Hamming distance-based multiprobing variant (HM) (12) (Table 3 2nd vs. 3rd column, second row).

Figure 5 shows the results for HM and CM, with different values r and b, and single probing strategy. We make the following observations. **(1)** Single probing fails to span the full accuracy-efficiency trade-off curve across all datasets. The retrieved set is noticeably sparse at $k/C \geq 0.50$. These results highlight the necessity of multiprobing to achieve sufficient candidate coverage across varying levels of retrieval selectivity. **(2)** CM consistently achieves better trade-off than the corresponding variant of HM and single-probing strategy, while smoothly spanning the full range of retrieval selectivity. As b increases, its performance improves consistently but with diminishing gains, saturating beyond $b = 32$. This indicates that a moderate number of co-occurrence-based token expansions suffices to approach near-exhaustive token expansion performance. **(3)** HM retrieves a broader range of candidates and spans the selectivity axis more effectively than the base impact score. However, as the Hamming radius r increases, the expansion becomes increasingly data-agnostic, ignoring semantic alignment from Impact_ψ. This leads to degraded MAP at large r.

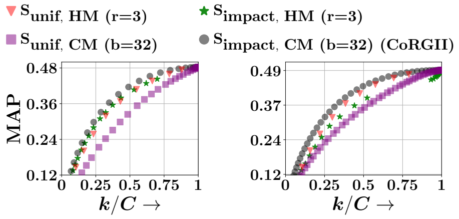

(a) PTC-FR (b) PTC-FM

Figure 7: Ablation on impact weight network

Effect of impact weighting network Next, we analyze the effect of impact weight network, by comparing with the variants of our model for both co-occurrence based multiprobing (CM, Eq. (14)) and Hamming distance based multiprobing (HM, Eq. (12)). This results in four models whose scores are $S_{\text{unif,HM}}$, $S_{\text{Impact,HM}}$, $S_{\text{unif,CM}}$ and $S_{\text{Impact,CM}}$ (CoRGII). Figure 7 summarizes the results. We observe that addition of impact weighting network improves the quality of trade-off, with significant performance gains observed for co-occurrence based multiprobing.

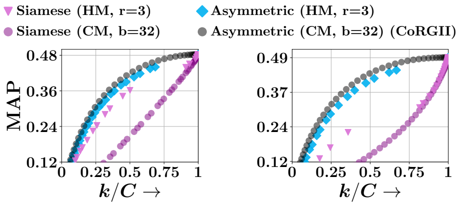

(a) PTC-FR (b) PTC-FM

Figure 9: Siamese vs Asymmetric architecture

Siamese vs Asymmetric architecture As discussed in Section 3.1, GTNet employs an asymmetric network architecture, which enables exact token matching while capturing the inherent asymmetry of subgraph matching. Here, we investigate its benefits by comparing against a Siamese variant of GTNet, which shares the same MLP across query and corpus graphs. Figure 9 summarizes the results for both co-occurrence based multiprobing (Eq. (14)) and Hamming based multiprobing (Eq. (12)) We highlight the following key observations: **(1)** The asymmetric variant of GTNet consistently outperforms the Siamese variant for both HM and CM. The performance boost is strikingly high for CM. **(2)** When using the asymmetric network, CM gives notable improvements over HM. However, for the Siamese variant, CM performs poorly on both PTC-FR and PTC-FM, while HM also suffers significantly on PTC-FM. This contrast highlights the importance of architectural asymmetry, especially for effective co-occurrence-based token matching.

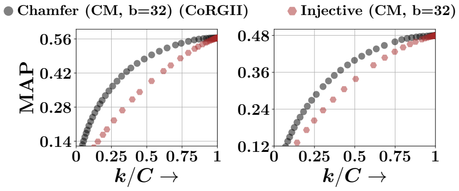

(a) COX2 (b) PTC-MR

Figure 10: Injective vs. Chamfer

Chamfer distance vs injective mapping Chamfer distance provides a non-injective mapping. Here, we compare its performance against traditional graph matching distance with injective mapping, *i.e.*, $\|\boldsymbol{Z}_q - \boldsymbol{P}\boldsymbol{Z}_c\|_1$, where $\boldsymbol{P}$ is a soft permutation (doubly stochastic) matrix. Figure 10 shows that Chamfer distance outperforms injective alignment-based graph matching. This

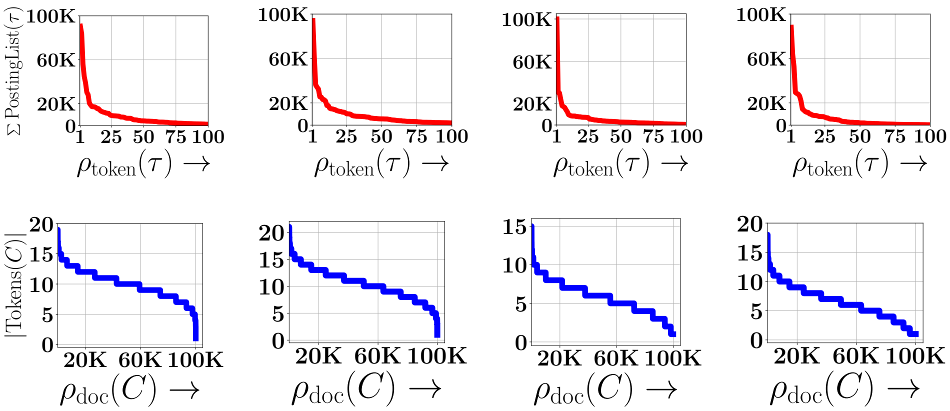

(a) PTC-FR (b) PTC-FM (c) COX2 (d) PTC-MR

Figure 11: Top row: Posting list length vs descending token rank. Bottom row: Number of unique tokens vs descending document rank. $\rho_{\text{token}}(\tau)$ represents the rank of the token τ when sorted in descending order of posting list lengths. $\rho_{\text{doc}}(C)$ is the rank of the document C when sorted in descending order of unique token count.

is because injective mappings tightly couple corpus embeddings $\boldsymbol{Z}_c$ with query embeddings $\boldsymbol{Z}_q$ preventing effective inverted indexing.

Token rank vs Document frequency We rank each token in the vocabulary by the length of its posting list, $\sum$ PostingList(τ), in descending order. Similarly, we rank each document by the number of unique tokens it contains, i.e., |Tokens(C)|.

In the top row of Figure 11, we plot the posting list lengths of tokens by rank. A small number of high-frequency tokens are associated with nearly all documents in the whole corpus, while the vast majority of tokens have short posting lists. The distribution exhibits a steep drop-off with rank, reminiscent of a Zipfian pattern. Inverted indexes are expected to be efficient in precisely these settings. In the second row, we plot the 'fill' of documents against documents ranked by their fills. A similar decay trend is observed, showing that most documents have a small number of tokens with non-zero impacts. Appendix G.4 contains more results.

5 Conclusion

We proposed CORGII, a scalable graph retrieval framework that bridges highly accurate late interaction query containment scoring with the efficiency of inverted indices. By discretizing node embeddings into structure-aware discrete tokens, and learning contextual impact scores, CORGII enables fast and accurate retrieval. Experiments show that CORGII consistently outperforms several baselines. Our work opens up several avenues of future work. It would be interesting to incorporate richly attributed graphs, capturing temporal dynamics in evolving corpora, learning adaptive token vocabularies, and exploring differentiable indexing mechanisms for end-to-end training. Another avenue is to integrate CORGII into large retrieval-augmented systems that require structured subgraph reasoning at scale.

6 Acknowledgements

Pritish acknowledges funding from the Qualcomm Innovation Fellowship. Indradyumna acknowledges funding from the Google PhD Fellowship and the Microsoft Research India PhD Award. Abir acknowledges funding from grants given by Amazon and Google, and the Bhide Family Chair Endowment Fund. Soumen acknowledges funding from Amazon and IBM, and the Halepete Family Chair Fund.

References

[1] Bingqing Lyu, Lu Qin, Xuemin Lin, Lijun Chang, and Jeffrey Xu Yu. Scalable supergraph search in large graph databases. In *2016 IEEE 32nd International Conference on Data Engineering (ICDE)*, pages 157–168, 2016. doi: 10.1109/ICDE.2016.7498237.

[2] Robert P Sheridan and Simon K Kearsley. Why do we need so many chemical similarity search methods? *Drug discovery today*, 7(17):903–911, 2002.

[3] Xiang Ling, Lingfei Wu, Saizhuo Wang, Gaoning Pan, Tengfei Ma, Fangli Xu, Alex X Liu, Chunming Wu, and Shouling Ji. Deep graph matching and searching for semantic code retrieval. *ACM Transactions on Knowledge Discovery from Data (TKDD)*, 15(5):1–21, 2021.

[4] Justin Johnson, Ranjay Krishna, Michael Stark, Li-Jia Li, David Shamma, Michael Bernstein, and Li Fei-Fei. Image retrieval using scene graphs. In *Proceedings of the IEEE conference on computer vision and pattern recognition*, pages 3668–3678, 2015.

[5] Donatello Conte, Pasquale Foggia, Carlo Sansone, and Mario Vento. Thirty years of graph matching in pattern recognition. *International journal of pattern recognition and artificial intelligence*, 18(03):265–298, 2004.

[6] Zhaoyu Lou, Jiaxuan You, Chengtao Wen, Arquimedes Canedo, Jure Leskovec, et al. Neural subgraph matching. *arXiv preprint arXiv:2007.03092*, 2020.

[7] Rishabh Ranjan, Siddharth Grover, Sourav Medya, Venkatesan Chakaravarthy, Yogish Sabharwal, and Sayan Ranu. Greed: A neural framework for learning graph distance functions. In *Advances in Neural Information Processing Systems 36: Annual Conference on Neural Information Processing Systems 2022, NeurIPS 2022*, 2022.

[8] Yujia Li, Chenjie Gu, Thomas Dullien, Oriol Vinyals, and Pushmeet Kohli. Graph matching networks for learning the similarity of graph structured objects. In *International conference on machine learning*, pages 3835–3845. PMLR, 2019.

[9] Indradyumna Roy, Venkata Sai Velugoti, Soumen Chakrabarti, and Abir De. Interpretable Neural Subgraph Matching for Graph Retrieval. *AAAI*, 2022.

[10] Ashwin Ramachandran, Vaibhav Raj, Indradyumna Roy, Soumen Chakrabarti, and Abir De. Iteratively refined early interaction alignment for subgraph matching based graph retrieval. *Advances in Neural Information Processing Systems*, 37:77593–77629, 2024.

[11] Wei Zhuo and Guang Tan. Efficient graph similarity computation with alignment regularization. *Advances in Neural Information Processing Systems*, 35:30181–30193, 2022.

[12] Aliaksei Severyn and Alessandro Moschitti. Learning to rank short text pairs with convolutional deep neural networks. In *Proceedings of the 38th International ACM SIGIR Conference on Research and Development in Information Retrieval*, SIGIR '15, page 373–382, New York, NY, USA, 2015. Association for Computing Machinery. ISBN 9781450336215. doi: 10.1145/2766462.2767738.

[13] Zhe Dong, Jianmo Ni, Dan Bikel, Enrique Alfonseca, Yuan Wang, Chen Qu, and Imed Zitouni. Exploring dual encoder architectures for question answering. In Yoav Goldberg, Zornitsa Kozareva, and Yue Zhang, editors, *Proceedings of the 2022 Conference on Empirical Methods in Natural Language Processing*, pages 9414–9419, Abu Dhabi, United Arab Emirates, December 2022. Association for Computational Linguistics. doi: 10.18653/v1/2022.emnlp-main.640. URL `https://aclanthology.org/2022.emnlp-main.640/`.

[14] Vladimir Karpukhin, Barlas Oguz, Sewon Min, Patrick Lewis, Ledell Wu, Sergey Edunov, Danqi Chen, and Wen-tau Yih. Dense passage retrieval for open-domain question answering. In Bonnie Webber, Trevor Cohn, Yulan He, and Yang Liu, editors, *Proceedings of the 2020 Conference on Empirical Methods in Natural Language Processing (EMNLP)*, pages 6769–6781, Online, November 2020. Association for Computational Linguistics. doi: 10.18653/v1/2020.emnlp-main.550.

[15] Omar Khattab and Matei Zaharia. Colbert: Efficient and effective passage search via contextualized late interaction over bert. In *Proceedings of the 43rd International ACM SIGIR conference on research and development in Information Retrieval*, pages 39–48, 2020.

[16] Gerard Salton. *Modern information retrieval*. McGraw-Hill, 1983.

[17] C.D. Manning, P. Raghavan, and H. Schütze. *Introduction to Information Retrieval*. Cambridge University Press, 2008. ISBN 9780521865715.

[18] Ricardo Baeza-Yates and Berthier Ribeiro-Neto. *Modern Information Retrieval*. ACM Press, 2nd edition, 1999.

[19] Otis Gospodnetic, Erik Hatcher, and Michael McCandless. *Lucene in action*. Simon and Schuster, 2010.

[20] Clinton Gormley and Zachary Tong. *ElasticSearch: The definitive guide: a distributed real-time search and analytics engine*. O'Reilly Media, Inc., 2015.

[21] Jimmy Lin, Xueguang Ma, Sheng-Chieh Lin, Jheng-Hong Yang, Ronak Pradeep, and Rodrigo Nogueira. Pyserini: A python toolkit for reproducible information retrieval research with sparse and dense representations. In *Proceedings of the 44th International ACM SIGIR Conference on Research and Development in Information Retrieval*, SIGIR '21, page 2356–2362, New York, NY, USA, 2021. Association for Computing Machinery. ISBN 9781450380379. doi: 10.1145/3404835.3463238.

[22] Jingdong Wang, Heng Tao Shen, Jingkuan Song, and Jianqiu Ji. Hashing for similarity search: A survey. *arXiv preprint arXiv:1408.2927*, 2014.

[23] Yu A Malkov and Dmitry A Yashunin. Efficient and robust approximate nearest neighbor search using hierarchical navigable small world graphs. *IEEE transactions on pattern analysis and machine intelligence*, 42(4):824–836, 2018.

[24] Ruiqi Guo, Philip Sun, Erik Lindgren, Quan Geng, David Simcha, Felix Chern, and Sanjiv Kumar. Accelerating large-scale inference with anisotropic vector quantization. In *International Conference on Machine Learning*, pages 3887–3896. PMLR, 2020.

[25] Matthijs Douze, Alexandr Guzhva, Chengqi Deng, Jeff Johnson, Gergely Szilvasy, Pierre-Emmanuel Mazaré, Maria Lomeli, Lucas Hosseini, and Hervé Jégou. The faiss library. *arXiv preprint arXiv:2401.08281*, 2024.

[26] Aristides Gionis, Piotr Indyk, Rajeev Motwani, et al. Similarity search in high dimensions via hashing. In *Vldb*, volume 99, pages 518–529, 1999.

[27] Scott Deerwester, Susan T Dumais, George W Furnas, Thomas K Landauer, and Richard Harshman. Indexing by latent semantic analysis. *Journal of the American society for information science*, 41(6):391–407, 1990.

[28] Christos Faloutsos and Douglas W Oard. *A survey of information retrieval and filtering methods*. Citeseer, 1995.

[29] Harsha Vardhan Simhadri, Ravishankar Krishnaswamy, Gopal Srinivasa, Suhas Jayaram Subramanya, Andrija Antonijevic, Dax Pryce, David Kaczynski, Shane Williams, Siddarth Gollapudi, Varun Sivashankar, Neel Karia, Aditi Singh, Shikhar Jaiswal, Neelam Mahapatro, Philip Adams, Bryan Tower, and Yash Patel. DiskANN: Graph-structured indices for scalable, fast, fresh and filtered approximate nearest neighbor search, 2023. URL `https://github.com/Microsoft/DiskANN`.

[30] Alexandr Andoni and Piotr Indyk. Near-optimal hashing algorithms for approximate nearest neighbor in high dimensions. *Communications of the ACM*, 51(1):117–122, 2008.

[31] Alexandr Andoni and Ilya Razenshteyn. Optimal data-dependent hashing for approximate near neighbors. In *Proceedings of the forty-seventh annual ACM symposium on Theory of computing*, pages 793–801, 2015.

[32] Alexandr Andoni, Piotr Indyk, Thijs Laarhoven, Ilya Razenshteyn, and Ludwig Schmidt. Practical and optimal lsh for angular distance. *Advances in neural information processing systems*, 28, 2015.

[33] Cong Fu, Chao Xiang, Changxu Wang, and Deng Cai. Fast approximate nearest neighbor search with the navigating spreading-out graph. *arXiv preprint arXiv:1707.00143*, 2017.

[34] Wen Li, Ying Zhang, Yifang Sun, Wei Wang, Mingjie Li, Wenjie Zhang, and Xuemin Lin. Approximate nearest neighbor search on high dimensional data—experiments, analyses, and improvement. *IEEE Transactions on Knowledge and Data Engineering*, 32(8):1475–1488, 2019.

[35] Ainesh Bakshi, Piotr Indyk, Rajesh Jayaram, Sandeep Silwal, and Erik Waingarten. A near-linear time algorithm for the chamfer distance, 2023. URL `https://arxiv.org/abs/2307.03043`.

[36] Keshav Santhanam, Omar Khattab, Christopher Potts, and Matei Zaharia. Plaid: an efficient engine for late interaction retrieval. In *Proceedings of the 31st ACM International Conference on Information & Knowledge Management*, pages 1747–1756, 2022.

[37] Thibault Formal, Benjamin Piwowarski, and Stéphane Clinchant. Splade: Sparse lexical and expansion model for first stage ranking. In *Proceedings of the 44th International ACM SIGIR Conference on Research and Development in Information Retrieval*, pages 2288–2292, 2021.

[38] Marco Cuturi. Sinkhorn distances: Lightspeed computation of optimal transport. *Advances in neural information processing systems*, 26:2292–2300, 2013.

[39] Gonzalo Mena, David Belanger, Scott Linderman, and Jasper Snoek. Learning latent permutations with gumbel-sinkhorn networks. *arXiv preprint arXiv:1802.08665*, 2018. URL `https://arxiv.org/pdf/1802.08665.pdf`.

[40] Number of simple connected graphs on n unlabeled nodes. Online. URL `https://oeis.org/A001349`.

[41] Christopher Morris, Nils M Kriege, Franka Bause, Kristian Kersting, Petra Mutzel, and Marion Neumann. Tudataset: A collection of benchmark datasets for learning with graphs. *arXiv preprint arXiv:2007.08663*, 2020.

[42] Indradyumna Roy, Rishi Agarwal, Soumen Chakrabarti, Anirban Dasgupta, and Abir De. Locality sensitive hashing in fourier frequency domain for soft set containment search. *Advances in Neural Information Processing Systems*, 36:56352–56383, 2023.

[43] Tomas Mikolov, Ilya Sutskever, Kai Chen, Greg S Corrado, and Jeff Dean. Distributed representations of words and phrases and their compositionality. *Advances in neural information processing systems*, 26, 2013.

[44] Jeffrey Pennington, Richard Socher, and Christopher D Manning. Glove: Global vectors for word representation. In *Proceedings of the 2014 conference on empirical methods in natural language processing (EMNLP)*, pages 1532–1543, 2014.

[45] Jacob Devlin, Ming-Wei Chang, Kenton Lee, and Kristina Toutanova. Bert: Pre-training of deep bidirectional transformers for language understanding. In *Proceedings of the 2019 conference of the North American chapter of the association for computational linguistics: human language technologies, volume 1 (long and short papers)*, pages 4171–4186, 2019.

[46] Herve Jegou, Matthijs Douze, and Cordelia Schmid. Product quantization for nearest neighbor search. *IEEE transactions on pattern analysis and machine intelligence*, 33(1):117–128, 2010.

[47] Vaibhav Raj, Indradyumna Roy, Ashwin Ramachandran, Soumen Chakrabarti, and Abir De. Charting the design space of neural graph representations for subgraph matching. In *The Thirteenth International Conference on Learning Representations*, 2025.

[48] Indradyumna Roy, Soumen Chakrabarti, and Abir De. Maximum common subgraph guided graph retrieval: late and early interaction networks. *Advances in Neural Information Processing Systems*, 35:32112–32126, 2022.

[49] Eeshaan Jain, Indradyumna Roy, Saswat Meher, Soumen Chakrabarti, and Abir De. Graph edit distance with general costs using neural set divergence. *Advances in Neural Information Processing Systems*, 37:73399–73438, 2024.

[50] Indradyumna Roy, Eeshaan Jain, Saswat Meher, Soumen Chakrabarti, and Abir De. Graph edit distance with general costs using neural set divergence. In *The Third Learning on Graphs Conference*, 2024.

[51] Indradyumna Roy, Saswat Meher, Eeshaan Jain, Soumen Chakrabarti, and Abir De. Position: Graph matching systems deserve better benchmarks. In *Forty-second International Conference on Machine Learning Position Paper Track*.

[52] Yu A Malkov and Dmitry A Yashunin. Efficient and robust approximate nearest neighbor search using hierarchical navigable small world graphs. *IEEE transactions on pattern analysis and machine intelligence*, 42(4):824–836, 2018.

[53] Antonella Falini. A review on the selection criteria for the truncated SVD in data science applications. *Journal of Computational Mathematics and Data Science*, 5:100064, 2022.

[54] Jure Leskovec, Anand Rajaraman, and Jeffrey David Ullman. *Mining of massive data sets*. Cambridge University Press, 2020.

[55] Sihao Yu, Jiafeng Guo, Ruqing Zhang, Yixing Fan, Zizhen Wang, and Xueqi Cheng. A re-balancing strategy for class-imbalanced classification based on instance difficulty. In *Proceedings of the IEEE/CVF conference on computer vision and pattern recognition*, pages 70–79, 2022.

[56] Jiaan Luo, Feng Hong, Jiangchao Yao, Bo Han, Ya Zhang, and Yanfeng Wang. Revive re-weighting in imbalanced learning by density ratio estimation. *Advances in Neural Information Processing Systems*, 37:79909–79934, 2024.

[57] Noga Alon, Dmitrii Avdiukhin, Dor Elboim, Orr Fischer, and Grigory Yaroslavtsev. Optimal sample complexity of contrastive learning. *arXiv preprint arXiv:2312.00379*, 2023.

[58] Lee Xiong, Chenyan Xiong, Ye Li, Kwok-Fung Tang, Jialin Liu, Paul Bennett, Junaid Ahmed, and Arnold Overwijk. Approximate nearest neighbor negative contrastive learning for dense text retrieval. *arXiv preprint arXiv:2007.00808*, 2020.

[59] Yingqi Qu, Yuchen Ding, Jing Liu, Kai Liu, Ruiyang Ren, Wayne Xin Zhao, Daxiang Dong, Hua Wu, and Haifeng Wang. Rocketqa: An optimized training approach to dense passage retrieval for open-domain question answering. *arXiv preprint arXiv:2010.08191*, 2020.

[60] Luyu Gao, Zhuyun Dai, and Jamie Callan. Coil: Revisit exact lexical match in information retrieval with contextualized inverted list. *arXiv preprint arXiv:2104.07186*, 2021.

[61] Tianyu Gao, Xingcheng Yao, and Danqi Chen. Simcse: Simple contrastive learning of sentence embeddings. *arXiv preprint arXiv:2104.08821*, 2021.

[62] Jianmo Ni, Chen Qu, Jing Lu, Zhuyun Dai, Gustavo Hernandez Abrego, Ji Ma, Vincent Y Zhao, Yi Luan, Keith B Hall, Ming-Wei Chang, et al. Large dual encoders are generalizable retrievers. *arXiv preprint arXiv:2112.07899*, 2021.

NeurIPS Paper Checklist

1. **Claims**

   Question: Do the main claims made in the abstract and introduction accurately reflect the paper's contributions and scope?

   Answer: [Yes]

   Justification: We claim that we have developed a novel indexing and retrieval system for graphs over a latent vocabulary, with sparse binary codes. The rest of the paper provides experiments and data to corroborate these claims. Please see figure 1 for an overview of the system, and section 4 for results.

   Guidelines:

   - The answer NA means that the abstract and introduction do not include the claims made in the paper.
   - The abstract and/or introduction should clearly state the claims made, including the contributions made in the paper and important assumptions and limitations. A No or NA answer to this question will not be perceived well by the reviewers.
   - The claims made should match theoretical and experimental results, and reflect how much the results can be expected to generalize to other settings.
   - It is fine to include aspirational goals as motivation as long as it is clear that these goals are not attained by the paper.

2. **Limitations**

   Question: Does the paper discuss the limitations of the work performed by the authors?

   Answer: [Yes]

   Justification: We provide the limitations in Appendix section B.

   Guidelines:

   - The answer NA means that the paper has no limitation while the answer No means that the paper has limitations, but those are not discussed in the paper.
   - The authors are encouraged to create a separate "Limitations" section in their paper.
   - The paper should point out any strong assumptions and how robust the results are to violations of these assumptions (e.g., independence assumptions, noiseless settings, model well-specification, asymptotic approximations only holding locally). The authors should reflect on how these assumptions might be violated in practice and what the implications would be.
   - The authors should reflect on the scope of the claims made, e.g., if the approach was only tested on a few datasets or with a few runs. In general, empirical results often depend on implicit assumptions, which should be articulated.
   - The authors should reflect on the factors that influence the performance of the approach. For example, a facial recognition algorithm may perform poorly when image resolution is low or images are taken in low lighting. Or a speech-to-text system might not be used reliably to provide closed captions for online lectures because it fails to handle technical jargon.
   - The authors should discuss the computational efficiency of the proposed algorithms and how they scale with dataset size.
   - If applicable, the authors should discuss possible limitations of their approach to address problems of privacy and fairness.
   - While the authors might fear that complete honesty about limitations might be used by reviewers as grounds for rejection, a worse outcome might be that reviewers discover limitations that aren't acknowledged in the paper. The authors should use their best judgment and recognize that individual actions in favor of transparency play an important role in developing norms that preserve the integrity of the community. Reviewers will be specifically instructed to not penalize honesty concerning limitations.

3. **Theory assumptions and proofs**

   Question: For each theoretical result, does the paper provide the full set of assumptions and a complete (and correct) proof?

   Answer: [NA]

   Justification: We do not include theoretical results in this paper.

   Guidelines:

   - The answer NA means that the paper does not include theoretical results.

- All the theorems, formulas, and proofs in the paper should be numbered and cross-referenced.
- All assumptions should be clearly stated or referenced in the statement of any theorems.
- The proofs can either appear in the main paper or the supplemental material, but if they appear in the supplemental material, the authors are encouraged to provide a short proof sketch to provide intuition.
- Inversely, any informal proof provided in the core of the paper should be complemented by formal proofs provided in appendix or supplemental material.
- Theorems and Lemmas that the proof relies upon should be properly referenced.

4. **Experimental result reproducibility**

   Question: Does the paper fully disclose all the information needed to reproduce the main experimental results of the paper to the extent that it affects the main claims and/or conclusions of the paper (regardless of whether the code and data are provided or not)?

   Answer: [Yes]

   Justification: We provide code, configurations/hyperparameters and instructions on how to run our experiments in the supplementary. Additionally, we provide the hyperparameters to our experiments in the main paper.

   Guidelines:

   - The answer NA means that the paper does not include experiments.
   - If the paper includes experiments, a No answer to this question will not be perceived well by the reviewers: Making the paper reproducible is important, regardless of whether the code and data are provided or not.
   - If the contribution is a dataset and/or model, the authors should describe the steps taken to make their results reproducible or verifiable.
   - Depending on the contribution, reproducibility can be accomplished in various ways. For example, if the contribution is a novel architecture, describing the architecture fully might suffice, or if the contribution is a specific model and empirical evaluation, it may be necessary to either make it possible for others to replicate the model with the same dataset, or provide access to the model. In general. releasing code and data is often one good way to accomplish this, but reproducibility can also be provided via detailed instructions for how to replicate the results, access to a hosted model (e.g., in the case of a large language model), releasing of a model checkpoint, or other means that are appropriate to the research performed.
   - While NeurIPS does not require releasing code, the conference does require all submissions to provide some reasonable avenue for reproducibility, which may depend on the nature of the contribution. For example
     (a) If the contribution is primarily a new algorithm, the paper should make it clear how to reproduce that algorithm.
     (b) If the contribution is primarily a new model architecture, the paper should describe the architecture clearly and fully.
     (c) If the contribution is a new model (e.g., a large language model), then there should either be a way to access this model for reproducing the results or a way to reproduce the model (e.g., with an open-source dataset or instructions for how to construct the dataset).
     (d) We recognize that reproducibility may be tricky in some cases, in which case authors are welcome to describe the particular way they provide for reproducibility. In the case of closed-source models, it may be that access to the model is limited in some way (e.g., to registered users), but it should be possible for other researchers to have some path to reproducing or verifying the results.

5. **Open access to data and code**

   Question: Does the paper provide open access to the data and code, with sufficient instructions to faithfully reproduce the main experimental results, as described in supplemental material?

   Answer: [Yes]

   Justification: We provide the link of these items.

   Guidelines:

   - The answer NA means that paper does not include experiments requiring code.
   - Please see the NeurIPS code and data submission guidelines (`https://nips.cc/public/guides/CodeSubmissionPolicy`) for more details.

- While we encourage the release of code and data, we understand that this might not be possible, so “No” is an acceptable answer. Papers cannot be rejected simply for not including code, unless this is central to the contribution (e.g., for a new open-source benchmark).
- The instructions should contain the exact command and environment needed to run to reproduce the results. See the NeurIPS code and data submission guidelines (`https://nips.cc/public/guides/CodeSubmissionPolicy`) for more details.
- The authors should provide instructions on data access and preparation, including how to access the raw data, preprocessed data, intermediate data, and generated data, etc.
- The authors should provide scripts to reproduce all experimental results for the new proposed method and baselines. If only a subset of experiments are reproducible, they should state which ones are omitted from the script and why.
- At submission time, to preserve anonymity, the authors should release anonymized versions (if applicable).
- Providing as much information as possible in supplemental material (appended to the paper) is recommended, but including URLs to data and code is permitted.

6. **Experimental setting/details**
   Question: Does the paper specify all the training and test details (e.g., data splits, hyperparameters, how they were chosen, type of optimizer, etc.) necessary to understand the results?
   Answer: [Yes]
   Justification: These details are provided in the experiments section 4 and will be included in greater detail in Appendix section F.
   Guidelines:
   - The answer NA means that the paper does not include experiments.
   - The experimental setting should be presented in the core of the paper to a level of detail that is necessary to appreciate the results and make sense of them.
   - The full details can be provided either with the code, in appendix, or as supplemental material.
7. **Experiment statistical significance**
   Question: Does the paper report error bars suitably and correctly defined or other appropriate information about the statistical significance of the experiments?
   Answer: [No]
   Justification: Error bars are not required in our experiments. This is because we have provided scatter plots where each point represents data collected from the experiment run for a separate configuration, for a wide variety of configurations. That is, our plot data is not in the form of aggregates.
   Guidelines:
   - The answer NA means that the paper does not include experiments.
   - The authors should answer "Yes" if the results are accompanied by error bars, confidence intervals, or statistical significance tests, at least for the experiments that support the main claims of the paper.
   - The factors of variability that the error bars are capturing should be clearly stated (for example, train/test split, initialization, random drawing of some parameter, or overall run with given experimental conditions).
   - The method for calculating the error bars should be explained (closed form formula, call to a library function, bootstrap, etc.)
   - The assumptions made should be given (e.g., Normally distributed errors).
   - It should be clear whether the error bar is the standard deviation or the standard error of the mean.
   - It is OK to report 1-sigma error bars, but one should state it. The authors should preferably report a 2-sigma error bar than state that they have a 96% CI, if the hypothesis of Normality of errors is not verified.
   - For asymmetric distributions, the authors should be careful not to show in tables or figures symmetric error bars that would yield results that are out of range (e.g. negative error rates).
   - If error bars are reported in tables or plots, The authors should explain in the text how they were calculated and reference the corresponding figures or tables in the text.
8. **Experiments compute resources**

Question: For each experiment, does the paper provide sufficient information on the computer resources (type of compute workers, memory, time of execution) needed to reproduce the experiments?

Answer: [Yes]

Justification: These details have been provided in experiments.

Guidelines:

- The answer NA means that the paper does not include experiments.
- The paper should indicate the type of compute workers CPU or GPU, internal cluster, or cloud provider, including relevant memory and storage.
- The paper should provide the amount of compute required for each of the individual experimental runs as well as estimate the total compute.
- The paper should disclose whether the full research project required more compute than the experiments reported in the paper (e.g., preliminary or failed experiments that didn't make it into the paper).

9. **Code of ethics**

   Question: Does the research conducted in the paper conform, in every respect, with the NeurIPS Code of Ethics `https://neurips.cc/public/EthicsGuidelines`?

   Answer: [Yes]

   Justification: The research conducted follows the ethics guidelines laid out by NeurIPS.

   Guidelines:

   - The answer NA means that the authors have not reviewed the NeurIPS Code of Ethics.
   - If the authors answer No, they should explain the special circumstances that require a deviation from the Code of Ethics.
   - The authors should make sure to preserve anonymity (e.g., if there is a special consideration due to laws or regulations in their jurisdiction).

10. **Broader impacts**

    Question: Does the paper discuss both potential positive societal impacts and negative societal impacts of the work performed?

    Answer: [Yes] ,

    Justification: Provided in Appendix A.

    Guidelines:

    - The answer NA means that there is no societal impact of the work performed.
    - If the authors answer NA or No, they should explain why their work has no societal impact or why the paper does not address societal impact.
    - Examples of negative societal impacts include potential malicious or unintended uses (e.g., disinformation, generating fake profiles, surveillance), fairness considerations (e.g., deployment of technologies that could make decisions that unfairly impact specific groups), privacy considerations, and security considerations.
    - The conference expects that many papers will be foundational research and not tied to particular applications, let alone deployments. However, if there is a direct path to any negative applications, the authors should point it out. For example, it is legitimate to point out that an improvement in the quality of generative models could be used to generate deepfakes for disinformation. On the other hand, it is not needed to point out that a generic algorithm for optimizing neural networks could enable people to train models that generate Deepfakes faster.
    - The authors should consider possible harms that could arise when the technology is being used as intended and functioning correctly, harms that could arise when the technology is being used as intended but gives incorrect results, and harms following from (intentional or unintentional) misuse of the technology.
    - If there are negative societal impacts, the authors could also discuss possible mitigation strategies (e.g., gated release of models, providing defenses in addition to attacks, mechanisms for monitoring misuse, mechanisms to monitor how a system learns from feedback over time, improving the efficiency and accessibility of ML).

11. **Safeguards**

    Question: Does the paper describe safeguards that have been put in place for responsible release of data or models that have a high risk for misuse (e.g., pretrained language models, image generators, or scraped datasets)?

    Answer: [NA]

    Justification: Our work does not pose such risks of misuse.

Guidelines:

- The answer NA means that the paper poses no such risks.
- Released models that have a high risk for misuse or dual-use should be released with necessary safeguards to allow for controlled use of the model, for example by requiring that users adhere to usage guidelines or restrictions to access the model or implementing safety filters.
- Datasets that have been scraped from the Internet could pose safety risks. The authors should describe how they avoided releasing unsafe images.
- We recognize that providing effective safeguards is challenging, and many papers do not require this, but we encourage authors to take this into account and make a best faith effort.

12. **Licenses for existing assets**

    Question: Are the creators or original owners of assets (e.g., code, data, models), used in the paper, properly credited and are the license and terms of use explicitly mentioned and properly respected?

    Answer: [Yes]

    Justification: We have provided citations wherever possible to any baseline or dataset that we have used in this paper. We have also ensured license compliance.

    Guidelines:

    - The answer NA means that the paper does not use existing assets.
    - The authors should cite the original paper that produced the code package or dataset.
    - The authors should state which version of the asset is used and, if possible, include a URL.
    - The name of the license (e.g., CC-BY 4.0) should be included for each asset.
    - For scraped data from a particular source (e.g., website), the copyright and terms of service of that source should be provided.
    - If assets are released, the license, copyright information, and terms of use in the package should be provided. For popular datasets, `paperswithcode.com/datasets` has curated licenses for some datasets. Their licensing guide can help determine the license of a dataset.
    - For existing datasets that are re-packaged, both the original license and the license of the derived asset (if it has changed) should be provided.
    - If this information is not available online, the authors are encouraged to reach out to the asset's creators.

13. **New assets**

    Question: Are new assets introduced in the paper well documented and is the documentation provided alongside the assets?

    Answer: [Yes]

    Justification: We provide sufficient documentation for all our assets, including for e.g. code.

    Guidelines:

    - The answer NA means that the paper does not release new assets.
    - Researchers should communicate the details of the dataset/code/model as part of their submissions via structured templates. This includes details about training, license, limitations, etc.
    - The paper should discuss whether and how consent was obtained from people whose asset is used.
    - At submission time, remember to anonymize your assets (if applicable). You can either create an anonymized URL or include an anonymized zip file.

14. **Crowdsourcing and research with human subjects**

    Question: For crowdsourcing experiments and research with human subjects, does the paper include the full text of instructions given to participants and screenshots, if applicable, as well as details about compensation (if any)?

    Answer: [NA]

    Justification: This work does not involve crowdsourcing.

    Guidelines:

    - The answer NA means that the paper does not involve crowdsourcing nor research with human subjects.

- Including this information in the supplemental material is fine, but if the main contribution of the paper involves human subjects, then as much detail as possible should be included in the main paper.
- According to the NeurIPS Code of Ethics, workers involved in data collection, curation, or other labor should be paid at least the minimum wage in the country of the data collector.

15. **Institutional review board (IRB) approvals or equivalent for research with human subjects**

    Question: Does the paper describe potential risks incurred by study participants, whether such risks were disclosed to the subjects, and whether Institutional Review Board (IRB) approvals (or an equivalent approval/review based on the requirements of your country or institution) were obtained?

    Answer: [NA]

    Justification: This work does not involve crowdsourcing.

    Guidelines:

    - The answer NA means that the paper does not involve crowdsourcing nor research with human subjects.
    - Depending on the country in which research is conducted, IRB approval (or equivalent) may be required for any human subjects research. If you obtained IRB approval, you should clearly state this in the paper.
    - We recognize that the procedures for this may vary significantly between institutions and locations, and we expect authors to adhere to the NeurIPS Code of Ethics and the guidelines for their institution.
    - For initial submissions, do not include any information that would break anonymity (if applicable), such as the institution conducting the review.

16. **Declaration of LLM usage**

    Question: Does the paper describe the usage of LLMs if it is an important, original, or non-standard component of the core methods in this research? Note that if the LLM is used only for writing, editing, or formatting purposes and does not impact the core methodology, scientific rigorousness, or originality of the research, declaration is not required.

    Answer: [NA]

    Justification: LLMs are not utilized in core research in this work.

    Guidelines:

    - The answer NA means that the core method development in this research does not involve LLMs as any important, original, or non-standard components.
    - Please refer to our LLM policy (`https://neurips.cc/Conferences/2025/LLM`) for what should or should not be described.

Appendix

A Broader Impact

Graph retrieval is a key enabler in many real-world domains where structured relationships are central. Our work on CoRGII contributes to subgraph-based retrieval, offering benefits across a range of applications:

- **Drug discovery and molecular search:** Efficient subgraph containment enables rapid screening of compounds containing functional motifs, aiding in virtual screening pipelines.
- **Program analysis and code intelligence:** Retrieval over control-flow or abstract syntax graphs can improve vulnerability detection and semantic code search.
- **Scene understanding and vision-language systems:** Graph-based representations of scenes or object relationships benefit from scalable matching of structured queries.
- **Scientific knowledge extraction:** Structured retrieval over citation or concept graphs supports discovery in large corpora of scientific knowledge.

By enabling fast and accurate retrieval of graphs under substructure containment, our work has the potential to improve the scalability and responsiveness of systems that rely on structured search over large graph collections. The proposed method, CoRGII, contributes toward democratizing structure-aware search by bridging discrete indexing methods with neural representations, making such systems more accessible to low-resource settings where dense model inference may be prohibitive.

While CoRGII offers efficiency and interpretability advantages, like any retrieval system, it may raise concerns when applied to sensitive graph-structured data—such as personal social networks or proprietary molecular datasets—potentially risking privacy or intellectual property leakage. Moreover, since training relies on learned embeddings, there remains a possibility of inherited biases from the underlying data. Practitioners are advised to apply appropriate safeguards, including privacy-preserving techniques and fairness auditing, when deploying the system in sensitive domains.

B Limitations

While CoRGII demonstrates strong performance in scalable graph retrieval, several aspects offer room for further improvement. We outline them below as avenues for future exploration:

- **Static token vocabulary:** Our framework relies on a fixed latent vocabulary defined by binary token length. Learning adaptive or dynamic vocabularies could improve representation flexibility and efficiency.
- **Lack of support for attributed or heterogeneous graphs:** CoRGII currently operates on purely structural information. Extending the framework to incorporate rich node/edge attributes and heterogeneous graph types is a natural next step.
- **Limited handling of evolving corpora:** The inverted index assumes a static corpus. Incorporating update-friendly indexing or continual learning mechanisms would enable deployment in dynamic settings, such as codebases or scientific repositories.

Addressing these limitations can further improve the adaptability, expressivity, and deployment readiness of CoRGII in diverse graph-based retrieval settings.

C Clarifications

In this section, we provide few clarifications as follows.

- **Sparse vs dense representations**. In text retrieval, a "sparse" index is keyed on discrete tokens. Sparse text indexes use inverted posting lists [16, 17, 18], in which the number of document (IDs) is vastly smaller than the corpus size, hence the name "sparse". In contrast, in a "dense" text index [25, 26, 27, 28, 29, 30, 31, 32, 33, 34], a text encoder converts text into continuous vectors and then they are indexed. Such dense representations are used for IVF, LSH (e.g., FHN) or DiskANN. Dense indexes are larger and slower to navigate than inverted indexes.
- **Latent token structure and token collisions**. The latent vocabulary is structured in the form of a posting list matrix $\mathbf{PL} \in \{0,1\}^{1024\times 100K}$. Each row of this matrix represents a token and each column a corpus item. The tokens themselves are not interpretable as they usually are in text indexing. However, the expectation from our pipeline and training scheme is that distinctive

subgraph motifs will be mapped to the same or strongly correlated groups of tokens. It is possible that different nodes from different graphs are mapped onto the same latent token, based on initial dense representation characteristics. This is further expanded upon in Appendix G.4.

D Related Work

D.1 A Brief History of Text-based Retrieval Architectures

Early information retrieval (IR) systems for text, relied on sparse lexical matching using bag-of-words (BoW) representations. Documents were encoded as high-dimensional sparse vectors over a fixed vocabulary, with inverted indices mapping each term to its corresponding document sets. Statistical term-weighting schemes like TF-IDF and BM25 were used to estimate relevance, prioritizing terms that were both frequent within a document yet discriminative across the corpus. Decades of research culminated in highly optimized sparse retrieval systems, such as Lucene [19] and Elasticsearch [20], which remain industry standards for lexical search.

Despite their efficiency, lexical methods are fundamentally limited by their reliance on surface-level token matching, failing to capture deeper semantic similarity. To address this, dense neural IR models were proposed, using learned embeddings–initially static (e.g., Word2Vec [43], GloVe [44]) and later contextual (e.g., BERT [45])– to encode text into compact, low-dimensional vector spaces that support semantic retrieval. As these dense representations are incompatible with inverted indices, retrieval relies on Approximate Nearest Neighbor (ANN) search techniques such as LSH [22], HNSW [23], and IVF [46], with efficient implementations provided by libraries like FAISS [25] and ScaNN [24].

Early dense retrieval systems typically compressed entire texts into single-vector representations, but this proved suboptimal for longer inputs due to over-compression, which obscures token-level distinctions. This limitation motivated a shift toward multi-vector representations, which preserve token-level information and enable more precise semantic alignment. Architectures such as ColBERT [15] and PLAID [36] adopt late interaction mechanisms that allow scalable token-wise retrieval. However, these methods still rely on ANN search as a subroutine, which—despite its effectiveness in dense settings—is slower than inverted indexing in practice.

To bridge the gap between dense semantic modeling and efficient retrieval, recent work has revisited sparse representations through a neural lens. Sparse neural IR models seek to combine the semantic expressiveness of dense models with the scalability and efficiency of traditional inverted indices. Approaches like SPLADE [37] learn document-specific, term-weighted sparse vectors by projecting inputs onto a high-dimensional vocabulary space. Crucially, this space is not limited to surface-level input tokens; the model can activate latent or implicitly relevant terms through learned expansions, effectively enriching the document representation beyond what is explicitly present in the text. This allows for semantically-informed exact matching within classical IR frameworks, effectively narrowing the gap between dense retrieval and sparse indexing.

D.2 A Briefer History of Neural Graph-Containment Scoring Models

Graph containment—determining whether a query graph G_q is (approximately) embedded within a corpus graph G_c—has long been a central problem in graph-based search. Traditional methods rely on combinatorial algorithms and subgraph isomorphism solvers, which are computationally expensive and scale poorly to large graph corpora. To address this, recent neural methods propose differentiable surrogates for containment using graph neural networks (GNNs). Raj et al. [47] provides a comprehensive analysis on different design components of neural models for subgraph isomorphism.

NeuroMatch [6] introduced a Siamese GNN with a hinge loss over aggregated node embeddings, but its global pooling loses fine structural detail. IsoNet [9] addresses this by retaining node-level embeddings $\boldsymbol{H}_q, \boldsymbol{H}_c$, computing soft alignments via a Gumbel-Sinkhorn network to produce a doubly stochastic matrix $\boldsymbol{P}$, and scoring relevance using an asymmetric hinge loss $[\boldsymbol{H}_q - \boldsymbol{P}\boldsymbol{H}_c]_+$. This better models subgraph containment and achieves improved empirical performance. IsoNet++ [10] extends this with early-interaction message passing for richer local-global representation. However, both IsoNet and IsoNet++ require dense, pairwise alignment across the corpus, limiting scalability. [48, 49, 50] use similar approaches for other type of graph similarities. Other recent works, such as [11, 7, 8], model graph similarity via node-level interactions using matching networks or soft attention. While these approaches capture structural alignment to some extent, they are tailored for general-purpose similarity tasks, making them less suited for subgraph containment and less scalable to large graph corpora.

E Additional details about our model and training

E.1 Pre-trained backbone

We use Isonet [9] for final scoring mechanism. IsoNet has two components: (1) a GNN and (2) a permutation network. GNN comprises of feature initialization network F_1; a message computation network F_2 and an embedding update (or combination) network F_3. Specifically, for the query graph G_q, we execute L mesage passing layers as follows:

$$\boldsymbol{h}_{q,0}(u) = F_1(\text{Feature}(u)) \quad \text{for all } u \in V_q \tag{15}$$

$$\boldsymbol{h}_{q,k+1}(u) = F_3\left(\boldsymbol{h}_{q,k}(u); \sum_{v:(u,v)\in E} F_2(\boldsymbol{h}_{q,k}(u), \boldsymbol{h}_{q,k}(v))\right), \quad \text{for all } u \in V_q, k \in \{0,..,L-1\} \tag{16}$$

We use the same procedure to compute the embeddings $\boldsymbol{h}_{c,k}$ for corpus graphs. We collect these embeddings in $\boldsymbol{H}_q, \boldsymbol{H}_c \in \mathbb{R}^{m\times \dim_h}$. These embeddings are finally used fed into multilayer perceptron, followed by dot product, to obtain an affinity matrix $\text{MLP}(\boldsymbol{H}_q)\,\text{MLP}(\boldsymbol{H}_c)^\top$ which is then provided as input into a node alignment network to obtain $\boldsymbol{P}$. Given a temperature hyperparameter temp, this network outputs a soft-permutation matrix using Sinkhorn iterations [38].

$$\boldsymbol{P} = \text{Sinkhorn}(\text{MLP}(\boldsymbol{H}_q)\,\text{MLP}(\boldsymbol{H}_c)^\top/\text{temp}) \tag{17}$$

Gumbel-Sinkhorn network consists of iterative row-column normalization as follows:

$$\boldsymbol{P}_0 = \exp(\text{MLP}(\boldsymbol{H}_q)\,\text{MLP}(\boldsymbol{H}_c)^\top/\text{temp}) \tag{18}$$

$$\boldsymbol{P}_{t+1} = \text{RowNormalize}\left(\text{ColumnNormalize}(\boldsymbol{P}_t)\right) \quad 0 \le t \le T-1. \tag{19}$$

As $T \to \infty$ $\boldsymbol{P}_T$ approaches as doubly stochastic matrix and as temp $\to 0, T \to \infty$, the matrix $\boldsymbol{P}_T$ approaches a permutation matrix.

In our work, we set $\dim_h = 10$. Here, F_1 is 10-dimensional encoder; F_2 consists of a combination of a propagator layer with a hidden dimension of 20 and a GRU layer at the output, with final dimension 10; and F_3 consists of an aggregator layer with hidden dimension 20 and output dimension 10. The MLPs used in Sinkhorn network, are linear-ReLU-linear networks. Each MLP has a hidden layer of 25 dimensions, and the output is of 25 dimensions. Finally, we minimize the ranking loss to obtain the parameters of F_1, F_2 and F_3 (Eq. (15)– (16)); and MLP used in Eq. (19)

$$\sum_q \sum_{c_\oplus \in \mathcal{C}_{q\oplus}} \sum_{c_\ominus \in \mathcal{C}_{q\ominus}} \left[\Delta(G_q, G_{c_\oplus}) - \Delta(G_q, G_{c_\ominus}) + \text{Margin}\right]_+ . \tag{20}$$

We used a margin of 0.5. Note that Δ is *only* used in the final stage of ranking. In Sinkhorn network, we set the number of iterations $T = 10$ and temparature 0.1.

E.2 Details about CORGII

Architecture of GTNet **and** Impact_ψ The GNN in GTNet consists of same architecture as in Eqs. (15)– (16), with the same number of layers and hidden dimensions. Here, we set $\dim(\boldsymbol{x}_\bullet) = 10$. Each of the MLPs in GTNet, *i.e.*, $\text{MLP}_{\phi_1}, \text{MLP}_{\phi_2}$ in Eqs. (2) and (3) consist of a linear-ReLU-linear network with input dimension 10, hidden layer of size 64 and output dimension 10. Note that GTNet does not share any components with the pre-trained backbone.

MLP_ψ used in Eq. (8) to model the impact scorer admits a similar architecture as $\text{MLP}_{\phi_1}, \text{MLP}_{\phi_2}$. It consists of a linear-ReLU-linear network with input dimension 10, hidden layer of size 64 and output dimension 10.

Optimization and Early Stopping. We train both models using the Adam optimizer with a learning rate of 1×10^{-3} and a batch size of 3000. During GTNet training, early stopping is performed at the sub-epoch level (i.e., across batches) with a patience of 30 steps and validation every 30 steps. For Impact_ψ, early stopping is applied at the epoch level with a maximum of 20,000 epochs and patience set to 50. Validation is conducted every epoch, with a default tolerance threshold of 5×10^{-3}. In both cases, the model is evaluated using the score function aligned with its training objective.

Margin Hyperparameter Tuning. For the Chamfer-based ranking loss in Eq. (5), we experiment with margin values of $\{0.01, 0.1, 1.0, 10, 30\}$. The best-performing margins are 10 for PTC-FR and PTC-FM, and 30 for COX2 and PTC-MR. For the impact network loss in Eq. (10), tested margins include $\{0.01, 0.1, 1.0\}$. Margins of 0.01, 0.01, 1.0, and 0.1 work best for PTC-FR, PTC-FM, COX2, and PTC-MR, respectively.

Training Under Co-Occurrence Expansion. During training with co-occurrence multiprobing, the token neighborhood $\mathcal{N}_b(\widehat{z}_q(u))$ in Eq. (14) is replaced with the full vocabulary $\mathcal{T}$. This allows Impact_ψ to learn a relevance-aware importance score for every token. At retrieval time, top-b tokens are selected based on sim, using the learned impact scores.

Reproducibility. All experiments are run with a fixed random seed of 42 across libraries and frameworks. We leverage PyTorch's deterministic execution setting and CuBLAS workspace configuration to ensure reproducible execution.

F Additional details about experiments

Dataset	$\min(\lvert V_C\rvert)$	$\max(\lvert V_C\rvert)$	$\mathbb{E}[\lvert V_C\rvert]$	$\min(\lvert E_C\rvert)$	$\max(\lvert E_C\rvert)$	$\mathbb{E}[\lvert E_C\rvert]$
PTC-FR	16	25	18.68	15	28	20.16
PTC-FM	16	25	18.70	15	28	20.13
COX2	16	25	19.65	15	26	20.23
PTC-MR	16	25	18.71	15	28	20.17

(a) Corpus graph statistics.

Dataset	$\min(\lvert V_Q\rvert)$	$\max(\lvert V_Q\rvert)$	$\mathbb{E}[\lvert V_Q\rvert]$	$\min(\lvert E_Q\rvert)$	$\max(\lvert E_Q\rvert)$	$\mathbb{E}[\lvert E_Q\rvert]$	$\mathbb{E}[\frac{\lvert y=1\rvert}{\lvert y=0\rvert}]$
PTC-FR	6	15	12.64	6	15	12.41	0.11
PTC-FM	7	15	12.58	7	15	12.34	0.12
COX2	6	15	13.21	6	16	12.81	0.11
PTC-MR	6	15	12.65	7	15	12.41	0.12

(b) Query graph statistics and average positive-to-negative label ratio ($\mathbb{E}[\frac{|y=1|}{|y=0|}]$).

Table 12: Statistics of sampled subgraph datasets used in our experiments. Each dataset consists of 500 query graphs and 100,000 corpus graphs.

F.1 Datasets

All experiments are performed on the following datasets: PTC-FR, PTC-FM, COX2 and PTC-MR [9, 51]. From each dataset, we extract corpus and query graphs using the sampling procedure outlined in [9], such that $|\mathcal{C}| = 100000$ and $|\mathcal{Q}| = 500$. The queryset is split such that $|\mathcal{Q}_{\text{train}}| = 300$, $|\mathcal{Q}_{\text{dev}}| = 100$ and $|\mathcal{Q}_{\text{test}}| = 100$. Each dataset has its relevant statistics outlined in Table 12, including the minimum, maximum and average number of nodes and edges in both the corpus set and the queryset. Additionally, the table also lists the per-query average ratio of positive ground truth relationships to negative ground truth relationships.

F.2 Baselines

We provide a detailed description of each of the baselines used in our experiments.

FourierHashNet It is a Locality-sensitive Hashing (LSH) mechanism designed specifically for the set containment problem [42], applied to subgraph matching. In particular, it overcomes the weaknesses of symmetric relevance measures. Earlier work employed measures such as Jaccard similarity, cosine similarity and the dot product to compute similarity between a pair of items, which do not reflect the asymmetric nature of the problem. FHN, on the other hand, employs a hinge-distance guided dominance similarity measure, which is further processed using a Fourier transform into the frequency domain. The idea is to enable compatibility with existing fast LSH techniques by leveraging inner products in the frequency domain, while retaining asymmetric notion of relevance.

We adopt the original architecture and training settings of FourierHashNet [42] without modification. The model employs 10 sampled Fourier frequencies to compute learned asymmetric embeddings, which are then optimized using a binary cross-entropy loss over embedding vectors of dimension 10. The final hash representation consists of 64-bit codes. For training, we perform a full grid sweep over the hyperparameter configurations proposed in the original work, including all specified loss weights.

To study the trade-off between retrieval accuracy and index efficiency, we vary the number of hash table buckets at query time, ranging from 2^1 to 2^{60}.

IVF The FAISS library provides facilities for inverted file indexing (IVF) [25]. IVF clusters the corpus of vectors using a suitable quantization method. The quantization method produces centroid vectors for each corpus vector, and each centroid represents a cluster. Internally, the library stores the vectors assigned to each cluster in the form of (possibly compressed) contiguous postings lists. To search this construction, a query vector is transformed into its corresponding centroid to match with the given cluster. Depending on the number of probes argument given during search time, one may expand their search into multiple neighboring clusters. We implement single-vector and multi-vector variants of IVF.

Note that we use the `faiss.IndexFlatIP` as the quantizer and `faiss.IndexIVFFlat` as the indexer.

DiskANN To tackle the challenge of having to store search indices in memory for strong recall, DiskANN introduces efficient SSD-resident indices for billion-scale datasets [29]. To this end, the authors develop a graph construction algorithm inspired by methods such as HNSW [52], but which produce more compact graphs (smaller diameter). They construct smaller individual indices using this algorithm on overlapping portions of the dataset, and then merge them into a single all-encompassing index. These disk-resident indices can then be searched using standard techniques. One of the key benefits of DiskANN is that it requires modest hardware for the construction and probing of their disk-resident indices. We implement single-vector and multi-vector variants. Note that we test against the memory-resident version of DiskANN.

We employ a graph degree of 16, complexity level of 32, alpha parameter of 1.2 during indexing. During search, we use an initial search complexity of 2^{21}.

F.3 Evaluation metric

We report Mean Average Precision (MAP) and the average number of retrieved candidates to characterize the efficiency–accuracy tradeoff. Retrieved candidates are reranked using the pretrained alignment model for consistent evaluation. For a query q with relevant corpus set $\mathcal{C}_{q\oplus}$ and a retrieved ranking π_q, we define the average precision (AP) as

$$\frac{1}{|\mathcal{C}_{q\oplus}|}\sum_{r=1}^{|\pi_q|} \text{Prec@}r \cdot \text{rel}_q(r) \tag{21}$$

where $\text{rel}_q(r) \in \{0, 1\}$ indicates whether the r-th ranked item is relevant to q and Prec@r is the precision at rank r. MAP is the mean of AP over all queries. This formulation penalizes high precision with low recall, ensuring models are rewarded only when most number of relevant items are retrieved with high retrieval accuracy.

F.4 System configuration

All experiments were conducted on an in-house NAS server equipped with seven 48GB RTX A6000 GPUs respectively. All model training is done on GPU memory. Further, the server is equipped with 96-core CPU and a maximum storage of 20TB, and runs Debian v6.1. We found that this hardware was sufficient to train CORGII.

F.5 Licenses

Our code will be released under the MIT license. DiskANN, FAISS and FourierHashNet are all released under the MIT license.

G Additional experiments

We present additional experimental results covering the comparison between co-occurrence-based multiprobing (CM) and Hamming multiprobing (HM), the ablation study on the impact scorer Impact_ψ, and the effect of using a Siamese versus asymmetric architecture in GTNet. We also include supporting analyses on posting list statistics—such as token frequency distributions and posting list co-occurrence patterns—as well as extended results for various CORGII variants.

G.1 CM vs HM

Figure 5 in the main paper compares co-occurrence multiprobing (CM) with Hamming multiprobing (HM) on the PTC-FR and PTC-FM datasets. Here, we present additional results on the COX2 and PTC-MR datasets.

Figure 13 confirms that CORGII remains the best-performing method overall, though the gap between CM and HM narrows on PTC-MR. **(1)** On COX2, HM fails to sweep the entire selectivity axis; even with $r = 7$, it only reaches up to $k/C = 0.6$. **(2)** CM steadily improves with increasing b, approaching exhaustive coverage, and saturates beyond $b = 32$. **(3)** On PTC-MR, while the difference between HM ($r = 7$) and CM ($b = 32$) is less pronounced, HM still does not cover the full selectivity range. **(4)** The trends and conclusions drawn in Section 4.1 remain consistent across these datasets.

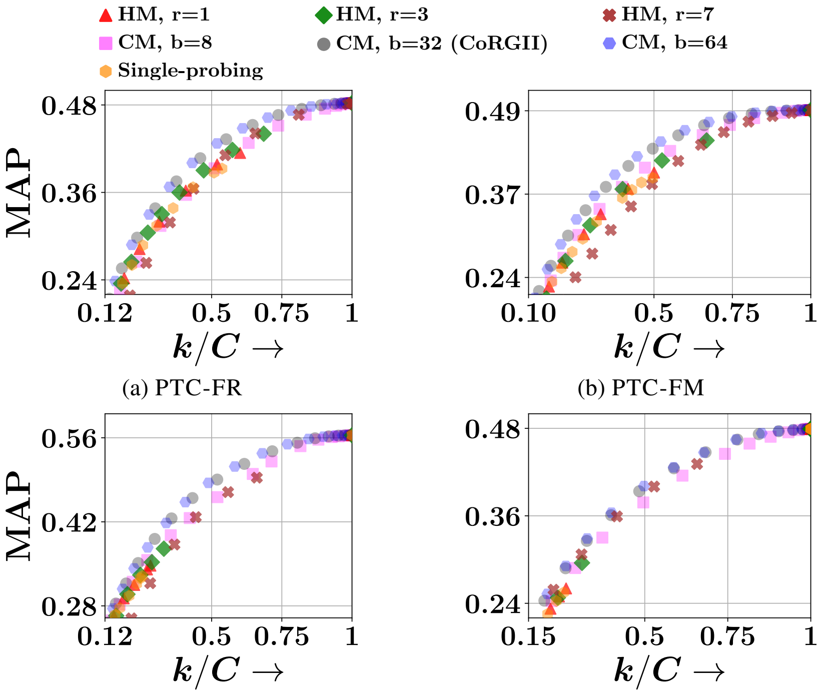

(a) PTC-FR

(b) PTC-FM

(c) COX2

(d) PTC-MR

Figure 13: Comparison of Hamming expansion multiprobing (HM) against co-occurrence expansion multiprobing (CM) across four real-world datasets and across several values of r (Hamming ball radius) and b (number of topmost co-occurring tokens). Each plot consists of tradeoffs between selectivity (k/C) and MAP, for different values of r and b. $b = 32$ is sufficient for CM to outperform HM variants. To deal with the crowding and overlapping problem in the plots, we have applied point sub-sampling on CORGII.

G.2 Impact weight network ablation

Figure 7 in the main paper examines the impact of the weighting network on the PTC-FR and PTC-FM datasets. We now extend this analysis to COX2 and PTC-MR in Figure 14, with the following observations: **(1)** CoRGII continues to outperform all other variants across the full retrieval budget spectrum on both datasets. **(2)** On COX2, uniform aggregation with Hamming multiprobing (HM) briefly approaches CoRGII at low k/C values, but quickly falls behind as selectivity increases. **(3)** Removing impact weights causes a significant drop in CM performance across both datasets, underscoring the value of learned token-level importance. **(4)** Uniform aggregation under CM fails to deliver competitive trade-offs, confirming that context-aware impact scoring is essential for effective retrieval.

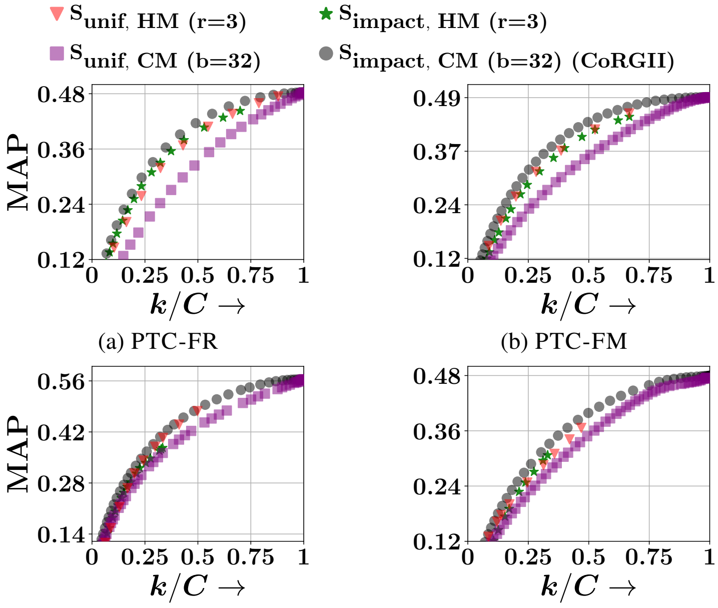

(a) PTC-FR

(b) PTC-FM

(c) COX2

(d) PTC-MR

Figure 14: Effect of ablation on the impact weight network across four datasets. Each subplot compares four retrieval variants: uniform aggregation with Hamming multiprobing ($S_{\text{unif, HM}}$), uniform aggregation with co-occurrence multiprobing ($S_{\text{unif, CM}}$), impact-weighted Hamming multiprobing ($S_{\text{impact, HM}}$), and impact-weighted co-occurrence multiprobing ($S_{\text{impact, CM}}$, the default CoRGII).

G.3 Siamese vs Asymmetric networks

Figure 9 in the main paper analyzes the contribution of CoRGII's asymmetric architecture on the PTC-FR and PTC-FM datasets. Figure 15 complements this analysis with results on COX2 and PTC-MR.

We observe: **(1)** CoRGII consistently outperforms both Siamese variants (with CM and HM probing), reaffirming the importance of architectural asymmetry for subgraph containment. **(2)** Among the HM variants, the asymmetric network achieves a better tradeoff curve compared to the Siamese counterpart, particularly evident in the mid-selectivity range. **(3)** Despite this, HM-based variants—both asymmetric and Siamese—fail to span the full selectivity axis, highlighting the limitations of Hamming multiprobing for recall. **(4)** These results further validate the need for asymmetry in the encoder architecture to accurately reflect containment semantics under both probing schemes.

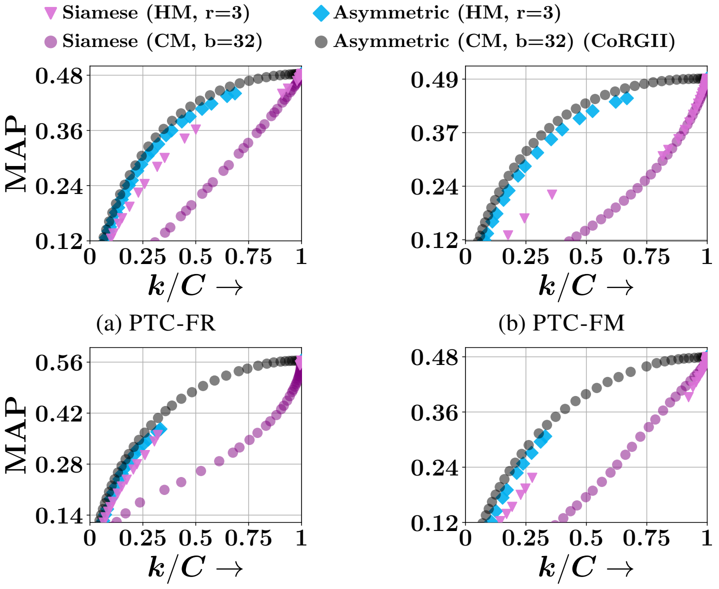

(a) PTC-FR

(b) PTC-FM

(c) COX2

(d) PTC-MR

Figure 15: Ablation comparing Siamese and asymmetric network architectures under different probing strategies. Each variant combines one of two network architectures—**Siamese** (shared MLP for query and corpus) and **Asymmetric** (separate MLPs)—with one of two probing strategies: **HM** (Hamming multiprobing with radius $r = 3$) or **CM** (Co-occurrence multiprobing with $b = 32$). CoRGII corresponds to the **Asymmetric + CM** configuration, shown as black circles.

G.4 Insights into token co-occurrence

Drawing parallels from natural language and retrieval systems, the structure of posting lists and corresponding token co-occurrence statistics are of key interest. In this section, we examine how these properties vary across datasets.

Co-occurrence statistics Table 16 reports structural statistics of the posting list matrix across all datasets. Let the posting list matrix be $\mathbf{PL} \in \{0,1\}^{1024 \times 100K}$, where each row represents a token and each column a document. The corresponding co-occurrence matrix is defined as $\mathbf{C} = \mathbf{PL} \cdot \mathbf{PL}^{\intercal} \in \mathbb{Z}_{+}^{1024 \times 1024}$.

We list both the *actual rank* and the *effective rank* of $\mathbf{PL}$, the latter computed using the energy-preserving criterion from truncated singular value decomposition (SVD) [53, 54]. Let $\sigma_1, \ldots, \sigma_n$ denote the singular values of $\mathbf{PL}$. The effective rank is the smallest K such that $\frac{\sum_{i=1}^{K} \sigma_i^2}{\sum_{i=1}^{n} \sigma_i^2} > \gamma$, with $\gamma = 0.95$. Since $\text{rank}(\mathbf{PL}) = \text{rank}(\mathbf{C})$ but $\text{rank}^{\text{eff}}(\mathbf{PL}) \geq \text{rank}^{\text{eff}}(\mathbf{C})$, the effective rank of $\mathbf{PL}$ serves as an informative upper bound for that of $\mathbf{C}$.

The large gap between the actual and effective rank across datasets—particularly the low effective rank—indicates that token co-occurrences lie on a low-dimensional manifold. This suggests that both $\mathbf{PL}$ and $\mathbf{C}$ are highly compressible, enabling projection onto a lower-dimensional subspace without significant loss of information. This again resembles the behavior of text corpora, where the discrete word space may be in the tens or hundreds of thousands, but a few hundred dense dimensions suffice to encode words and documents [27].

Dataset	Actual Rank	Effective Rank
PTC-FR	393	4
PTC-FM	498	9
COX2	250	7
PTC-MR	232	3

Table 16: Actual and effective rank (95% SVD energy threshold) of the posting list matrix $\mathbf{PL}$ for each dataset.

G.5 End-to-End Training vs Frozen Backbone for $\mathbf{S}_{\text{unif, CM}}$ and $\mathbf{S}_{\text{unif, HM}}$

A key design consideration is whether GTNet benefits from end-to-end training using its own GNN encoder, or whether comparable results can be obtained using frozen embeddings from a pretrained backbone. Figure 17 compares the performance of $\mathbf{S}_{\text{unif, CM}}$ and $\mathbf{S}_{\text{unif, HM}}$ under both configurations.

We observe that: **(1)** End-to-end training consistently yields better MAP–selectivity tradeoffs for both CM and HM variants, indicating that learning task-specific embeddings improves token discriminability. **(2)** The frozen backbone variant spans a wider range of selectivity values (k/C), suggesting looser token matching and higher recall, but at the cost of reduced precision. **(3)** End-to-end models tend to retrieve fewer candidates for the same threshold, reflecting tighter, more precise tokenization.

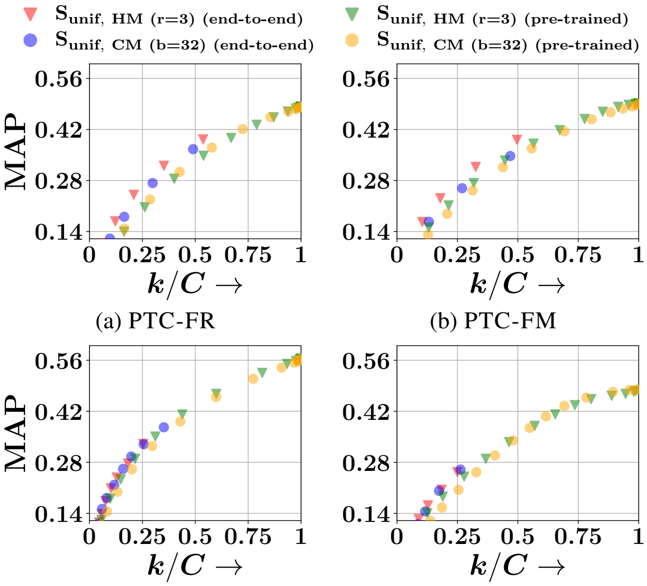

(a) PTC-FR (b) PTC-FM

(c) COX2 (d) PTC-MR

Figure 17: Comparison of end-to-end training versus using a frozen backbone for $\mathbf{S}_{\text{unif, CM}}$ and $\mathbf{S}_{\text{unif, HM}}$, with $r = 3$ and $b = 32$. End-to-end training refers to learning the GTNet encoder jointly, while the frozen variant reuses pretrained embeddings.

In the next set of ablations, we show that the impact network does not need pre-trained IsoNet embeddings of the given dataset to maintain superior tradeoffs.

G.6 Using pre-trained IsoNet embeddings of different dataset as input to Impact$_\psi$

Instead of using pre-trained IsoNet embeddings h on the same dataset, we use h trained on the PTC-FM dataset as input to the impact network for PTC-FR, and likewise use h trained on PTC-MR and apply to the impact network for COX2. Table 18 shows the efficiency in terms of fraction of graphs k/C retrieved to achieve atleast a certain MAP=m^*. Lower k/C is better and indicates higher efficiency. _ denotes places where the method is unable to achieve the target MAP.

G.7 Using intermediate embeddings x of GTNet as input to Impact$_\psi$

Next, instead of pre-trained embeddings h, we use x as input to the impact scoring model (Impact$_\psi(\tau, x)$), (8)), where x is the embedding from the GTNet GNN, (which is not pretrained and trained as a part of the CoRGII scheme).

The following Table 19 shows the efficiency in terms of fraction of graphs k/C retrieved to achieve atleast a certain MAP=m^* for PTC-FR (first subtable) and COX2 (second subtable) datasets. Lower k/C is better and indicates higher efficiency.

m^*	CoRGII		FHN		IVF	
	current	**(h trained on PTC-FM)**	**default**	**(h trained on PTC-FM)**	**default**	**(h trained on PTC-FM)**
0.38	0.38	0.42	0.51	0.97	0.76	0.81
0.40	0.44	0.47	0.81	1.0	0.89	0.81
0.45	0.645	0.69	0.99	1.0	0.96	0.91

(a) k/C values for **PTC-FR**.

m^*	CoRGII		FHN		IVF	
	current	**(h trained on PTC-MR)**	**default**	**(h trained on PTC-MR)**	**default**	**(h trained on PTC-MR)**
0.36	0.31	0.27	0.61	1.0	0.64	0.57
0.38	0.35	0.29	0.71	–	0.64	0.81
0.40	0.45	0.37	0.99	–	0.83	0.81

(b) k/C values for **COX2**.

Table 18: k/C values comparing CoRGII, FHN, and IVF with and without transferring h across datasets. CoRGII outperforms the baselines even when the pre-trained h of a different dataset is used.

m^*	CoRGII		FHN	DiskANN-multi	IVF-multi
	(current)	**(use x)**			
0.38	0.38	0.37	0.51	0.87	0.76
0.4	0.44	0.43	0.81	0.87	0.89
0.45	0.64	0.62	0.99	0.93	0.96

(a) k/C for **PTC-FR**.

m^*	CoRGII		FHN	DiskANN-multi	IVF-multi
	(current)	**(use x)**			
0.36	0.31	0.42	0.61	0.55	0.64
0.38	0.35	0.48	0.71	0.82	0.64
0.42	0.45	0.58	0.99	0.82	0.83

(b) k/C for **COX2**.

Table 19: k/C values comparing CoRGII (current h vs. using x), FHN, DiskANN-multi, and IVF-multi. CoRGII outperforms each of the baselines even when not using h as impact network input.

G.8 Using pre-trained Graph Embedding Network embeddings as input to Impact$_\psi$

We pre-train a different model called Graph Embedding Network (GEN) [8], which is different from the final reranking model. Table 20 contains the results, with _ denoting places where the method is unable to achieve target MAP:

m^*	Ours		FHN		DiskANN-multi		IVF-multi	
	(current)	**(pretrained GEN-embed.)**	**(current)**	**(pretrained GEN-embed.)**	**(current)**	**(pretrained GEN-embed.)**	**(current)**	**(pretrained GEN-embed.)**
0.38	0.38	0.38	0.51	1.0	0.87	0.82	0.76	0.82
0.40	0.44	0.44	0.81	–	0.87	0.88	0.89	0.94
0.45	0.64	0.65	0.99	–	0.93	0.98	0.96	0.94

(a) k/C for **PTC-FR**.

m^*	Ours		FHN		DiskANN-multi		IVF-multi	
	(current)	**(pretrained GEN-embed.)**	**(current)**	**(pretrained GEN-embed.)**	**(current)**	**(pretrained GEN-embed.)**	**(current)**	**(pretrained GEN-embed.)**
0.36	0.31	0.25	0.61	0.60	0.55	0.65	0.64	0.65
0.38	0.35	0.29	0.71	0.60	0.82	0.76	0.64	0.76
0.40	0.45	0.35	0.99	0.80	0.82	0.76	0.83	0.76

(b) k/C for **COX2**.

Table 20: k/C values comparing CoRGII, FHN, DiskANN-multi, and IVF-multi models under both current and pretrained GEN-embedding settings. CoRGII outperforms other methods when the impact network is not conditioned on pre-trained IsoNet embeddings.

G.9 Estimating the error of the Chamfer approximation

Final recall computation requires impact scoring and multiprobing. It would be useful to gauge the effect of the Chamfer approximation before getting to that stage. Towards this goal, we provide the following error-based estimator to evaluate the efficacy of the Chamfer approximation without measuring recall.

We compute ground-truth distance dist^*, distance $\mathrm{dist}_{\mathrm{soft}}$ under soft permutation, and Chamfer distance $\mathrm{dist}_{\mathrm{chamfer}}$ (see Equation 4):

$$\mathrm{dist}^* \;=\; \min_{\mathbf{P}} \sum_{i,j} \Big[\mathbf{A}_q - \mathbf{P}\,\mathbf{A}_c\,\mathbf{P}^\top\Big]_+[i,j]$$

$$\mathrm{dist}_{\mathrm{soft}} \;=\; \sum_{i,j} \Big[\mathbf{Z}_q - \mathbf{P}^{\mathrm{soft}}\mathbf{Z}_c\Big]_+[i,j]$$

The following Table 21 shows that dist^* is better approximated by $\mathrm{dist}_{\mathrm{chamfer}}$ than by $\mathrm{dist}_{\mathrm{soft}}$.

Dataset	$\mathrm{Average}(\lvert\mathrm{dist}^* - \mathrm{dist}_{\mathrm{soft}}\rvert)$	$\mathrm{Average}(\lvert\mathrm{dist}^* - \mathrm{dist}_{\mathrm{chamfer}}\rvert)$
PTC-FR	26.9	**20.18**
PTC-FM	35.42	**22.53**

Table 21: Chamfer better approximates dist^* (lower is better).

H Further discussion

In this section, we include further material of interest. Specifically, we include index memory and timing statistics for our method, a discussion on the generalizability of our impact scorer and a discussion on the sample complexity of contrastive learning.

H.1 Index memory and timing statistics

In the Table 22 below, we report index construction time and memory usage, both of which remain modest and practical across datasets, supporting the scalability of CORGII. Further, we observe that indexing of CORGII on the PTC-FR dataset takes 46M and 272s for a **million graphs**, which is quite modest.

Dataset	**Indexing time**	**Index memory**
PTC-FR	29s	3.6M
COX2	27.2s	4.3M

Table 22: Index construction time and memory usage for CORGII.

H.2 Discussion on generalizability of impact score function

Below, we discuss the effect of node types that may occur very infrequently in the corpus, and whether there may not be sufficiently many samples to guarantee good generalization of the learned impact score function Impact_ψ.

We emphasize that even if there are such rare graphs, we train the impact scorer using a ranking loss on the aggregated ranked list. Suppose we have relevant query–corpus pairs G_q and G_c, each with rare tokens. During the batching procedure, our ranking loss ensures that $S(G_q, G_c) > S(G_{q'}, G_{c'})$ whenever $G_{q'}$ and $G_{c'}$ are not relevant, including for graphs that have richly contextualized tokens. This allows the training algorithm to reinforce a strong enough signal into the impact scorer. If we use $S(G_q, G_c)$ as the sole scoring function, then we obtain a modest $\mathrm{MAP} \approx 0.28$ even if S is not any graph-matching model and is driven by a simple MLP.

This can be further enhanced by using the following modification of the impact scores:

$$\sum_{u \in V_q} \mathrm{Impact}_\psi\big(\hat{\mathbf{z}}_q(u), \mathbf{h}_q(u)\big)\, \mathbb{I}\big[\hat{\mathbf{z}}_q(u) \in \omega(G_c)\big] \;\longrightarrow\; \sum_{u \in V_q} \lambda\, \mathrm{Impact}_\psi\big(\hat{\mathbf{z}}_q(u), \mathbf{h}_q(u)\big)\, \mathbb{I}\big[\hat{\mathbf{z}}_q(u) \in \omega(G_c)\big]$$

Here, λ is a hyperparameter greater than 1 and is only applied if $\hat{\mathbf{z}}_q(u)$ is a rare token.

H.3 Discussion on sample complexity of contrastive learning

Here, we discuss the sample complexity of the contrastive learning methods that we have employed to train our pipeline (especially the impact scorer), in the context of relevant past work. Consider the resampling or re-balancing algorithm proposed in [55]. At each iteration t, we may use a sampling procedure, formulated as a multinomial distribution $\mathrm{Multinomial}(D^t)$ over all corpus items (with $D^t = [D^t_c : c \in C]$) over difficulty estimates D^t_c of tokenizing the graphs arising due to presence of rare tokens. Then, we re-train or fine-tune the tokenizer GTNet on graphs sampled from this distribution. In this case, we can compute predictions of tokens as $z^{(t)}(u)$ for each node u. Then, we leverage the prediction variations $z^{(t)}(u) - z^{(t-1)}(u)$ (and their signs) to compute difficulty for each node. Then, we can aggregate these difficulty values across nodes to compute difficulty $D^{(t)}_c$ for G_c. We can also compute

$$\sum_{u \in V_q} \mathrm{Impact}_\psi\big(\hat{\mathbf{z}}_q(u), \mathbf{h}_q(u)\big)\, \mathbb{I}\big[\hat{\mathbf{z}}_q(u) \in \omega(G_c)\big] \;\longrightarrow\; \sum_{u \in V_q} \lambda\, \mathrm{Impact}_\psi\big(\hat{\mathbf{z}}_q(u), \mathbf{h}_q(u)\big)\, \mathbb{I}\big[\hat{\mathbf{z}}_q(u) \in \omega(G_c)\big]$$

as a proxy difficulty per node. This would be a more principled alternative to our proposal in Section H.2 involving λ.

Next, the paper [56] assigns suitable weights $\alpha(x, y)$ on the loss per each instance. It would be an interesting research problem to design $\alpha(z(u), G_c)$ similar to [56]. A key challenge in immediately adapting [56] is that we may need to estimate $P(G_c \mid z(u))$ as used in Eq. (2) in [56], which would pose an interesting research question.

Discussion of Alon et al. [57] Contrastive training is ubiquitous in dense retrieval, starting from such classic papers as DPR [14], ANCE [58], and RocketQA [59]. Further enhancements were reported in COIL [60], SimCSE [61], and GTR [62]. Alon et al. [57] provide extremely insightful observations on the sampling complexity of contrastive learning from a PAC point of view. They show that, for contrastive training with n points in $\tilde{d}$-dimensional space, $\tilde{\Omega}(\min(nd, n^2))$ samples are needed. They provide two escape clauses, however. First, the number of samples needed reduces if the points admit some underlying clusters. Second, if each triplet comes with a demand for large separation, then the lower bound drops to $\tilde{\Omega}(n)$. In LSH-style retrieval, large separation is usually the goal, in the sense that points "near" the query should fall into the same bucket (Hamming distance 0) as the query, and "far" points (that are $\geq (1 + \epsilon)$ times farther than near points) should fall into other buckets (Hamming distance ≥ 1). It is possible that this is what makes contrastive training work well in retrieval applications.